

2

CR-102510

GRUMMAN



HAZARD DETECTION METHODS FOR A LUNAR ROVING VEHICLE

Final Report

FACILITY FORM 602

N70-27541
(ACCESSION NUMBER)

83
(PAGES)

CR-102510
(NASA CR OR TMX OR AD NUMBER)

(THRU)

(CODE)

11
(CATEGORY)



Reproduced by the
CLEARINGHOUSE
for Federal Scientific & Technical

JANUARY 1970

HAZARD DETECTION METHODS FOR A LUNAR ROVING VEHICLE

————— Final Report —————

Prepared for:

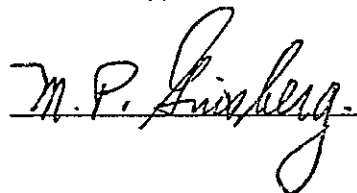
NATIONAL AERONAUTICS AND SPACE ADMINISTRATION
GEORGE C. MARSHALL SPACE FLIGHT CENTER—
HUNTSVILLE, ALABAMA 35812

CONTRACT NAS 8-25098
DCN 1-X-40-94302 (IF)

Prepared by:

J. Elefant, E. Lavan and E. Veshlage

Approved by:

A handwritten signature in black ink, appearing to read "M. P. Ginsberg", is written over a horizontal line.

GRUMMAN AEROSPACE CORPORATION
BETHPAGE, NEW YORK 11714

FOREWORD

This report was produced in accordance with NASA Contract NAS 8-25098 under the technical management of Lee Malone and in consultation with Donald Stone, NASA Astrionics Laboratory, George C. Marshall Space Flight Center, Alabama. It defines RF and Seismic techniques for detecting hazards to a Lunar Roving Vehicle in accordance with Exhibit A of the contract.

CONTENTS

<u>Section</u>		<u>Page</u>
1	Summary	1
2	Introduction	2
3	Conclusions	4
4	Literature Search	5
5	Surface Hazard Detection	7
	5.1 RF Techniques	7
	5.1.1 Antenna Location	8
	5.1.2 Antenna Beamwidth	8
	5.1.3 Transmitter Frequency	8
	5.1.4 Antenna Scanning	11
	5.1.5 Radiated Power Requirements	13
	5.1.6 Radar Candidate Systems	14
	5.1.7 Power and Weight Estimates	24
6	Sub-Surface Hazard Detection	25
	6.1 Seismic System	33
	6.2 Seismic Sources	35
	6.3 Configuration of Vehicle	37
	6.4 Soil Penetrating Radar	41
	6.5 Additional Techniques	47
7	System Impact on LRV	49
	7.1 Effect of System on Mission Requirements	49
	7.2 Compatibility of System with LRV Space, Weight and Power Requirements	50
	7.3 Ancillary Equipment Requirements	51
8	Recommendations	54
9	References	56
10	Bibliography	58
	APPENDIX A - Surface Hazard Detection Analyses	A-1

ILLUSTRATIONS

Figure		Page
1	Proposed Antenna and RF Sensor Location on LRV	9
2	Antenna Beam Geometry	10
3	Transverse Coverage with Six Beam Switched Antennas	12
4	Lunar Reflectivity vs Incidence Angle	15
5	FM-CW Radar Block Diagram	18
6	Simplified Pulse Radar Block Diagram	20
7	Seismic Refraction Shot	26
8	Seismic Refraction Shot	27
9	Seismic Reflection Shot	28
10	Seismic Reflection Shot	29
11	Gravity Hammer Rolling Seismic Source	36
12	Spring-Loaded Hammer Rolling Seismic Source	38
13	Spring-Loaded Hammer Seismic Source	39
14	Seismic Void Detectors on LRV	40
15	Decibel Loss per Meter for Low-Loss Dielectrics	44
16	Soil Absorption Loss vs Frequency	45
17	Soil Absorption Loss vs Frequency	46
18	Minimal Hazard Detection System	52
19	Vehicle Approaching 25° Slope	A-2
20	Vehicle Approaching One Meter Hole	A-4
21	Vehicle Approaching 35° Slope	A-6
22	Vehicle Approaching One Meter Block	A-7
23	Vehicle Approaching Change of Slope	A-15
24	Vehicle Approaching Change of Slope	A-16

1 - SUMMARY

This report contains the results of a study to define a system capable of detecting potential hazards to a lunar roving vehicle and preventing it from moving into a position which will prevent continuation of the mission. The study consisted of the following:

- A literature search of all pertinent areas and subjects to determine that any concept under consideration had not already been evaluated.
- Determination of sensor or combination of sensors to identify potential hazards. Techniques were limited to radio frequency wave propagation above or through the lunar surface and seismic wave propagation through the lunar surface.

Pulse and FM-CW radars were investigated as candidates for a surface hazard detection system. Preliminary choices of system parameters such as antenna configurations, beam width, depression angle and transmitting frequency were made. Analyses of errors inherent to the system and those contributed by the lunar terrain were made and approaches offered for minimizing these errors.

Seismic techniques and soil penetrating radar were investigated. Approaches and shortcomings of applying these techniques to a subsurface hazard detection system were analyzed.

- The basic information derived from the sensor investigations were used to determine the physical and performance impact on the LRV capability. Considerations were given to weight, power, space, mounting configurations, and ancillary equipment to support the hazard detection system.

2 - INTRODUCTION

Surface mobility is a fundamental requirement for continued lunar exploration beyond the initial Apollo landings. A lunar roving vehicle (LRV) will provide mobility for astronauts and will have the capability for performing long-range geological and geophysical traverses by remote control from the earth. In the remote control mode it will have a range of at least 1000 Km and a possible operational life of one year. Limitations will be imposed on the monitor and controller on earth due to TV bandwidth, limited field of view, absence of sound and motion cues, adverse lighting, communication disturbances, and the 2.6 second (minimum) communications time delay. Thus, it will be necessary to have a hazard detection and avoidance system aboard the LRV to prevent mission failure.

For the purpose of study the following surface discontinuities were defined as hazards:

- Surface holes having a diameter (horizontal measurement) greater than one meter and a depth greater than one meter.
- Rocks having a width (horizontal dimension) greater than one meter and/or a height (local vertical dimension) greater than one meter.
- Cracks or fractures in the surface, if they are wider or longer and in either case deeper than one meter.
- Surface crusts, concealing holes, too thin to support the weight of the LRV.

At the onset of the study NASA recommended that the investigation consider the space, weight and power guidelines established by Grumman's LRV project for a hazard detection system. These guidelines were established to be:

- Space less than 1 ft³
- Weight less than 10 pounds
- Power less than 10 watts

The discussion that follows begins with the results of a literature search of various concepts and techniques for hazard detection. This is followed by a section devoted to RF techniques for surface hazard detection. Seismic techniques and soil penetrating radar approaches to sub-surface hazard detection are then discussed. Finally, the impact that the proposed systems would have on the LRV is presented.

In addition to the main technical discussion, recommendations are made for further investigations in this area. Appendix A has been included to provide detailed analyses of errors effecting the RF approach to a hazard detection system.

3 - CONCLUSIONS

Surface hazards to the LRV can be detected by the candidate FM-CW radar system. The candidate system will meet the range and resolution requirements of the unmanned mission of the LRV for the majority of the lunar terrain expected to be traversed by the LRV. Errors due to certain lunar terrain configurations will produce false alarm rates, however compensation can be provided to minimize these errors.

Increases in space, weight and power beyond the present guidelines would be necessary to meet range and resolution requirements for speeds higher than the unmanned mode. In addition, the utilization of beamwidths in the order of one degree would be necessary to meet the resolution requirements.

At present sub-surface hazards exist only in theory. Analysis of recent lunar seismic data may provide evidence to support this theory. It will be extremely difficult to provide accurate advanced warning of sub-surface hazards. The seismic and soil penetrating radar techniques presented in this report offer approaches to this detection problem. However, the present state-of-the-art of these techniques requires the use of equipment whose size and weight would be extremely difficult to implement aboard a lunar roving vehicle. It is concluded that if sub-surface hazards continue to be matter of concern, research should be extended in these areas so that a practical system capable of being installed on the LRV might be developed.

4 - LITERATURE SEARCH

4.1 SOURCES

The main sources utilized were: NASA, Scientific and Technical Aerospace Reports (STAR), Defense Documentation Center, Technical Abstract Bulletins (TAB); International Aerospace Abstracts (IAA), and Government and industry publications located in Grumman's Engineering Library.

Computer print-out literature searches in the area of short-range radars and seismic detectors were received from NASA Scientific and Technical Information Facility. Pertinent information in the areas of RF and seismic detectors was received from equipment manufacturers via vendor conferences, catalogues and technical reports. Additional seismic information was obtained from the National Speleological Society Library.

4.2 LISTING OF REPORTS

All pertinent reports perused during the literature search are listed in this report. Those reports used as sources for the study analysis are listed in the reference section. Those reports which contain pertinent information but which were not directly used to support the analysis are listed in the bibliography section.

4.3 CONCLUSION ON STATE-OF-THE-ART FROM LITERATURE SEARCH

In the extensive literature search conducted by Grumman no RF or seismic system was found which could meet all of the hazard detection requirements of the lunar roving vehicle.

Numerous systems exist in the RF area which offer approaches for an RF hazard detection system. The most promising systems exist in the field of radar altimeters. A considerable part of the study effort was devoted to this approach and the findings are discussed in the section on RF sensors.

The literature on seismic sensors is devoted mainly to detection by passive means. Reports on active seismic schemes are devoted mainly to systems containing numerous arrays, large base lines and long-term detection analyses. However, some techniques

reported offer approaches which might be utilized to warn the LRV of sub-surface hazards. These approaches are discussed in the section on Seismic sensors.

The literature search also located many reports concerned with soil analysis and measurement of sub-surface stratification features utilizing RF techniques. Soil penetrating radar offers another approach to the detection of sub-surface hazards to the LRV. This approach is discussed in the section on soil penetrating radar.

5 - SURFACE HAZARD DETECTION

5.1 RF TECHNIQUES

This section of the report is devoted to RF techniques and the feasibility of adapting them to a hazard detection system for a lunar roving vehicle. The hazards of concern to the vehicle in this section are surface hazards and are defined as follows:

- Surface holes having a diameter (horizontal measurement) of one meter or larger and depth of at least one meter
- Rocks having a width (horizontal dimension) greater than one meter and height (local vertical dimension) greater than one meter.

These formations are considered negotiable limits to the LRV configuration used as the baseline for this study when the vehicle is travelling in the remote control or un-manned mode. The maximum vehicle speed in this mode is 2km/hr. In addition to the surface hazards defined above, power constraints on the baseline configuration set limits on slopes that the vehicle can negotiate. Thus, positive or negative slopes greater than 35° are also considered surface hazards.

The minimum detection distance requirement depends upon the type and slope of the terrain, the braking capability of the vehicle and the response time of the detection system. Consideration has been given to this requirement and is discussed further in the report.

For the purpose of clarity the investigation of RF techniques for surface hazard detection is presented in the following manner. Those parameters which are common to all techniques are presented first. Next, various candidate RF techniques are discussed and the most promising candidate selected.

In the application of RF techniques to a hazard detection system for a lunar roving vehicle numerous sources of error arise. These include discernment of slopes, effects of pitch and roll, lunar terrain roughness, change of slope, and inherent radar errors. The detailed discussion of these parameters has been included in Appendix A. Where applicable, the results of these analyses have been included in this section of the report.

5.1.1 Antenna Location

The LRV configuration used as the baseline for the study is shown in figure 1. In this configuration a mast structure has been provided for the TV camera and is also used for mounting the RF antenna. The mast is located on the centerline of the vehicle and 1.25 meters behind the wheelfront. The antenna is located as high as possible on the mast to increase the depression angle of the radar beam and to provide greater back scattering coefficient. It also has the advantage of an increase in the line of sight. Constraints imposed by free-space-loss, wave-guide plumbing losses, and increased errors due to pitch and roll, limit the height at the antennas to three meters above the terrain.

A minimum detection distance of 1.75 meters in advance of the wheelfront is required to enable the discernment of positive slopes of 35° or more (see Appendix A-1). This implies an antenna depression angle of 45° (see Fig. 2).

5.1.2 Antenna Beamwidth

The same antenna will be used for the detection of both holes (negative obstacles) and rocks (positive obstacles). The radar system employed measures slant range to the terrain, so that the range reading increases when a negative obstacle is detected and decreases when a positive obstacle is detected. To improve the capability of detecting any obstacle and for greater resolution in measuring range to the obstacle, it is desirable to keep the beamwidth smaller than the width of the obstacle. Narrower beamwidths will improve the gain and resolution, however, the size of the antenna will increase accordingly. Furthermore, too narrow a beamwidth may result in an increase in noise due to insufficient terrain averaging. A 5° elevation beamwidth will illuminate an approximate longitudinal distance of 1/2 meter (3 db points) centered about 1.75 meters in advance of the wheelfront (see Fig. 2). A 7.5° azimuth beamwidth provides approximately 1/2 meter transverse coverage.

5.1.3 Transmitter Frequency

The transmitter frequency determines the antenna size after the beamwidth has been selected. Higher frequencies reduce the size and weight of the antenna as well as that of the RF receiver and transmitter components. The highest frequency which should be used is limited by the reliability and availability of components, the available RF power output, and the lunar surface back scatter coefficient. This limit is reached in K-band between 15 and 30 Ghz. Operational solid state altimeters are available at 18 Ghz which weigh less than 4 pounds and uses less than 6 watts input power for 2000 ft. ranges at

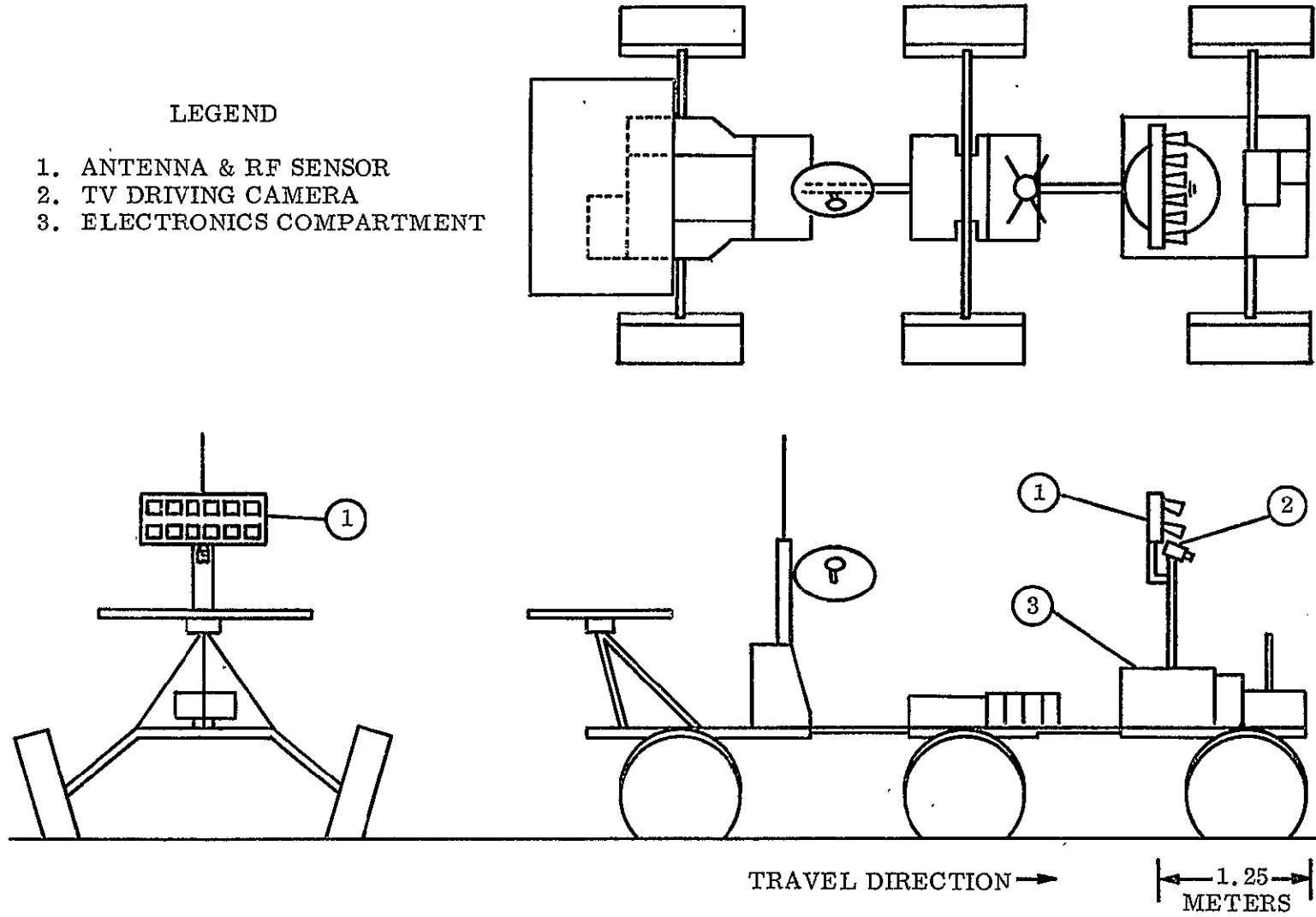
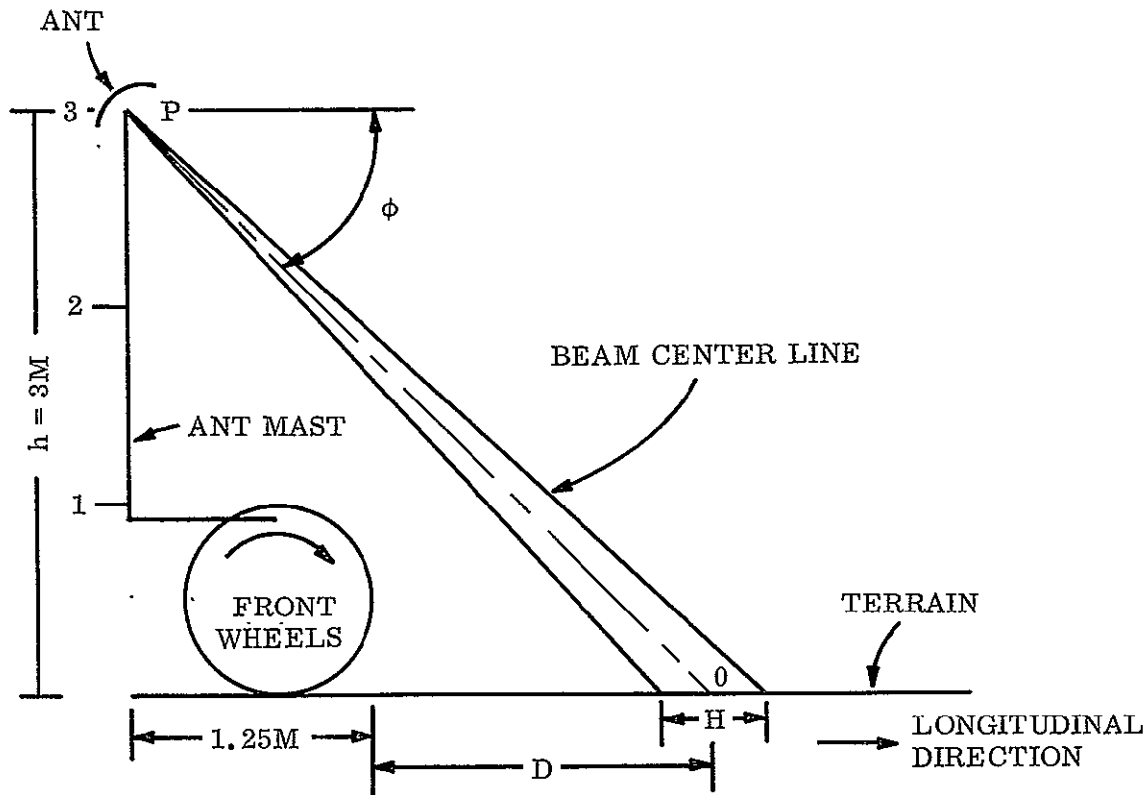


Figure 1. Proposed Antenna and RF Sensor Location on LRV



ELEVATION VIEW

θ = antenna beamwidth = 5°
 h = antenna height = 3 meters
 D = preceding illumination distance
 ϕ = depression angle = $\tan^{-1} \frac{h}{D+1.25}$

R = slant range (PO) = $\frac{D+1.25}{\cos \phi}$

H = longitudinal illumination = $\frac{R \phi}{\sin \phi}$

	ϕ	R Meters	H Meters
$D = 1.5M$	47.4°	4.06	.480
$D = 1.75M$	45°	4.25	.525
$D = 2.0M$	42.8°	4.42	.570

Figure 2. Antenna Beam Geometry

normal incidence (ref. 6). The final choice of frequency would be determined by a detailed study of hardware availability. A preliminary choice of 25 Ghz with a 5° x 7.5° beamwidth establishes the antenna size of 6.7" by 4.5".

5.1.4 Antenna Scanning

In order to obtain a margin of safety during maneuvering it is desirable to provide transverse coverage at least one and three quarters feet wider than the vehicle or a minimum of 146 inches (3.7 meters). To provide antenna coverage over the transverse range required will make an antenna scanning system a necessity. Two possible choices are:

- Multiple sampled fixed beam antennas with sequential processing for minimum hardware weight.
- Servo driven pencil beam antennas.

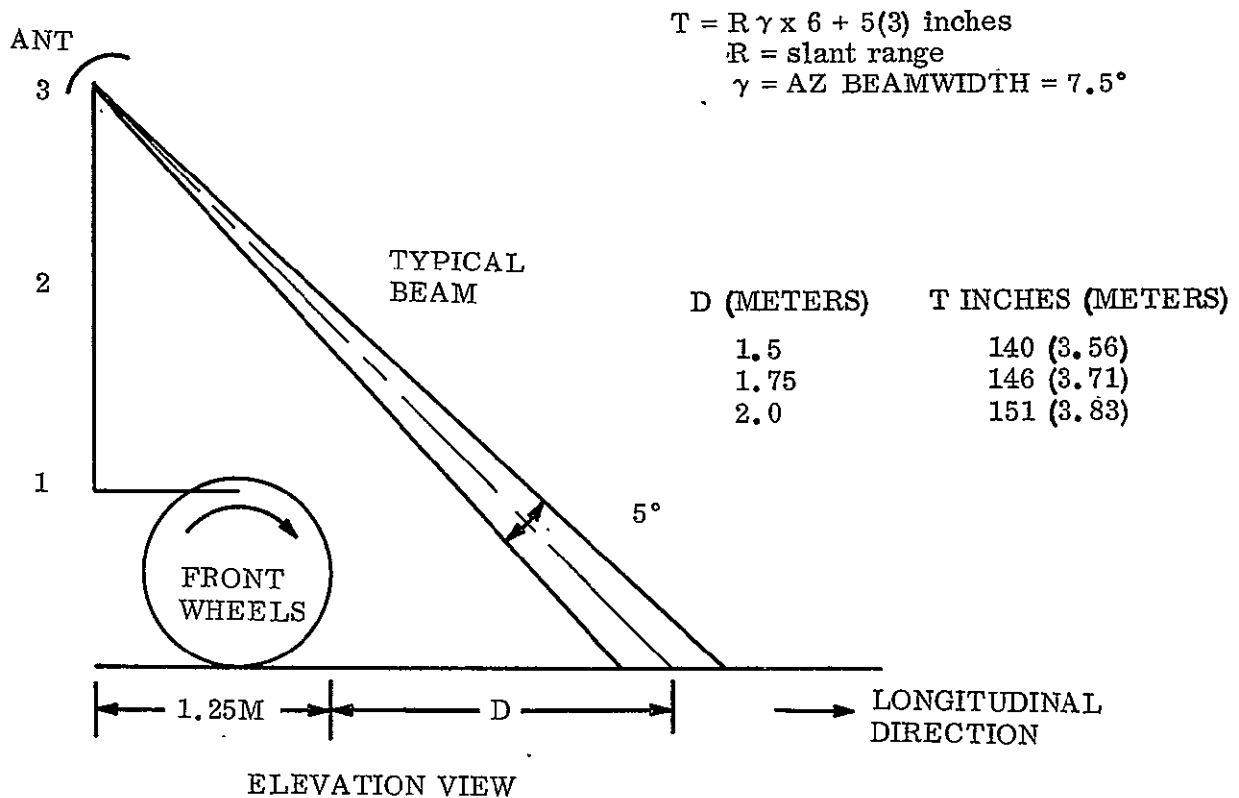
5.1.4.1 Multiple Sampled Fixed Beam Antennas

Using 7.5° azimuth beamwidth antennas, a total of six overlapping beams are required to provide the transverse coverage (Fig. 3). A single transmitter and receiver will be used to economize on hardware, weight and power requirements. The six antennas will be sampled with a switch. Diode switching of both the transmitter and receiver is feasible. Using an FM-CW system, separate receive and transmit antennas with a high degree of isolation are required for each beam. A pulsed carrier system would use a single antenna per beam for both transmission and reception. As shown in Appendix A-1, the information rate from each antenna must be at least one sample every half second or a maximum of every 1/4 meter of vehicle travel. A switching speed of 2 cycles per second will meet this requirement. Switching may be accomplished using diodes in shunt or in series with the antenna feeds. Since radar types such as FM-CW require separate transmit and receive antennas, they would require a total of 12 antennas and 12 switching diodes. Each receive antenna would be located approximately a foot below its associated transmit antenna in order to provide adequate isolation (Ref. 1).

5.1.4.2 Servo Driven Antenna

The servo driven antenna has many disadvantages such as:

- Requirement for long-life, high-vacuum bearings.
- Requirement for shielding against lunar dust.
- Increased power required for servo drives.



ELEVATION BEAMWIDTH = 5
 AZIMUTH BEAMWIDTH = 7.5

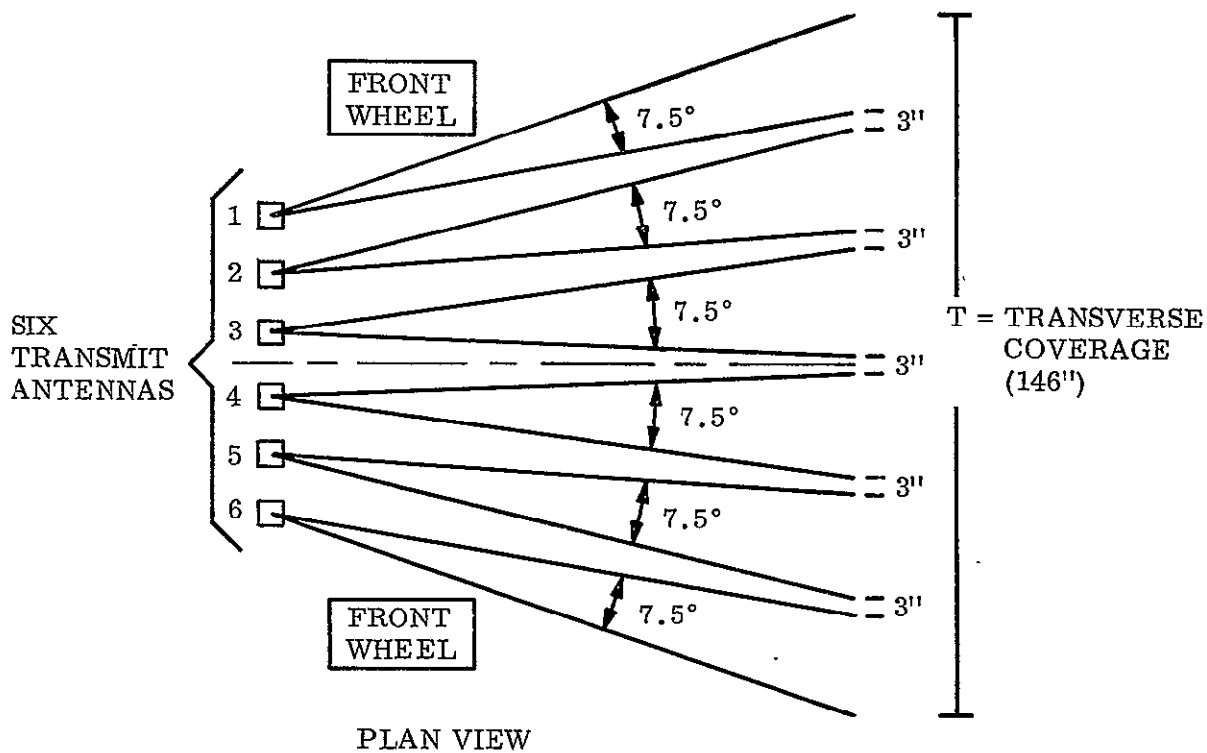


Figure 3. Transverse Coverage With Six Beam Switched Antennas

- Relatively low, long-term reliability for rotary components.
- Inability to increase reliability by the use of redundancy with respect to the mechanical components.

Its major advantage is that it requires only a single antenna or pair of antennas.

Based on the above considerations, a diode switched array of antennas has been tentatively selected as a preferred scanning system.

5.1.1.5 Radiated Power Requirements

The required power can be calculated by use of the following standard radar equations:

$$P_T = \frac{(4\pi)^3 R^4 P_R L}{G^2 \lambda^2 \sigma}$$

$$G \approx \frac{8.2}{\theta_E \theta_H}$$

$$\sigma = A \sigma_0 = (R \theta_E) (R \theta_H) \sigma_0$$

where:

P_T = Transmitter average power (milliwatts)

P_R = Receiver returned average power (milliwatts)

R = Slant range (meters)

G = Antenna gain

σ_0 = Radar backscatter cross-section (square meters)

θ_E = Antenna elevation plane beamwidth (radians)

θ_H = Antenna azimuth plane beamwidth (radians)

A = Illuminated area (square meters)

L = Microwave transmission losses

λ = RF wavelength (meters)

The assumed parameters are:

R = 4.25 meters

λ = .012 meters (for 25 Ghz)

$$\begin{aligned} \theta_E &= .087 \text{ radians } (5^\circ) \\ \theta_H &= .131 \text{ radians } (7.5^\circ) \\ \sigma_o &= 10^{-3} \text{ (-30 db)} \\ L &= 4 \text{ (6 db)} \\ P_R &= 10^{-9} \text{ milliwatts (-90 dbm)} \end{aligned}$$

σ_o is based on the measured Surveyor and Apollo data shown in Figure 4 (Ref. 2). Since this data was based on large patch sizes and was taken at X-band and Ku-band, it was modified by adding a 12 db safety factor to the measured σ_o . This 12 db allows for small patch size lunar terrain variability and represents a safety factor to cover the uncertainty involved.

P_R is based on the use of a receiver with an effective noise bandwidth of 0.5 Mhz, a noise figure of 12 db and a minimum discernible signal (MDS) of -90 dbm.

Substituting these values into the power equation, the minimum required transmitter average power is found:

$$P_T = \frac{(4\pi)^3 (4.25)^4 (4) 10^{-9}}{\left[\frac{8.2}{(.087) (.131)} \right]^2 \left[.012 \right]^2 \left[(4.25)^2 (.087) (.131) 10^{-3} \right]}$$

$$P_T \approx 0.17 \text{ milliwatts}$$

The use of a 10 milliwatt transmitter average power would provide a margin of approximately 18 db. This would allow for an operating S/N of 12 db and a 6 db margin for aging and environmental effects.

5.1.6 Radar Candidate Systems

Before discussing particular radar systems, it should be mentioned that the principles discussed previously have been general and will be applicable to all of the following radar system.

5.1.6.1 The FM-CW Candidate System

This system operates on the principle of the radar altimeter by transmitting an FM signal (using either sawtooth or sinusoidal modulation) and measuring the beat frequency between the transmitted and received signals. This frequency is proportional

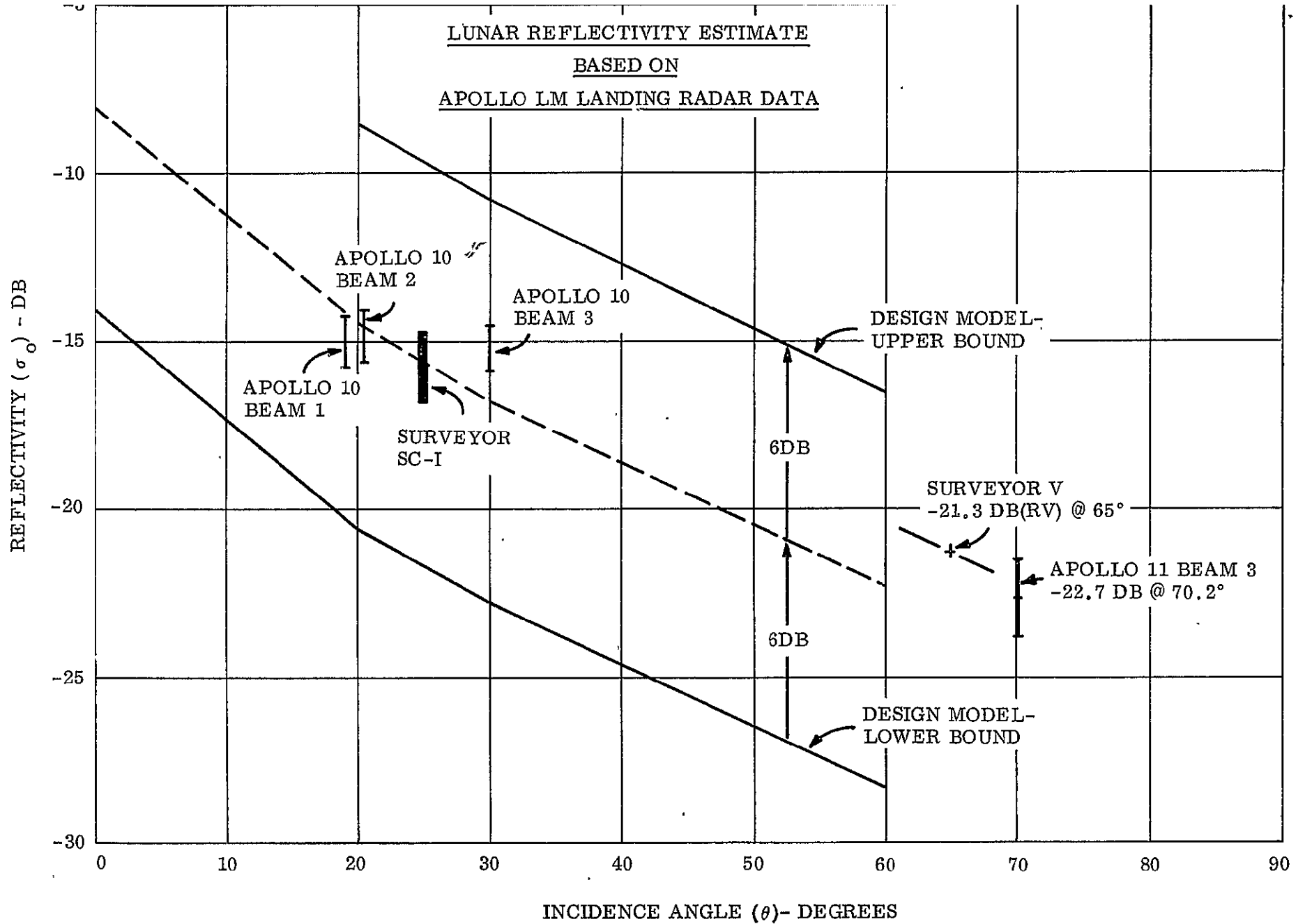


Figure 4. Lunar Reflectivity vs. Incidence Angle

to the range. Figure 5 is a block diagram of an FM-CW radar. For reference, some of the electrical values are:

Transmitter freq. = 25 ghz; IF freq. = 30 Mhz; IF amp. bandwidth = 0.5 Mhz;
 transmitter average output power = 10 MW; receiver sensitivity (MDS) = -90 dbm;
 receiver noise figure = 12 db.

The beat frequency f_B is given by:

$$f_B = \frac{4R f_m \Delta f}{C}$$

where R = slant range; C = velocity of light; f_m is the modulation frequency; and Δf is the frequency deviation.

For R = 4.25 meters; $f_m = 200$ hz; and $\Delta f = 135$ mhz

$$f_B = 1530 \text{ hz}$$

A source of error arises in systems utilizing cycle counting for frequency measurement. This error is called the quantizing or "fixed step error" which is due to the fact that the frequency counter will only count integral cycles of the beat frequency in the period $1/f_m$. This fixed step error is given by

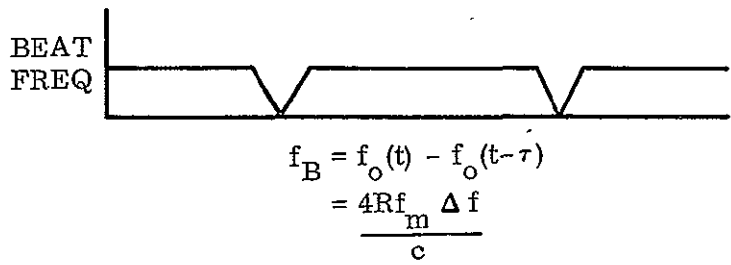
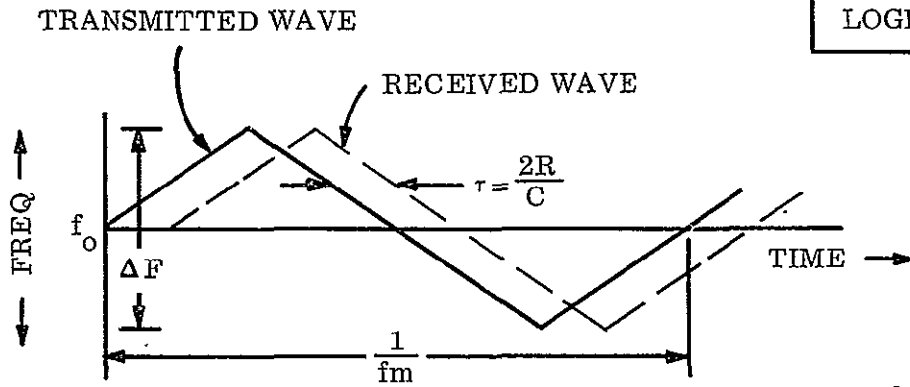
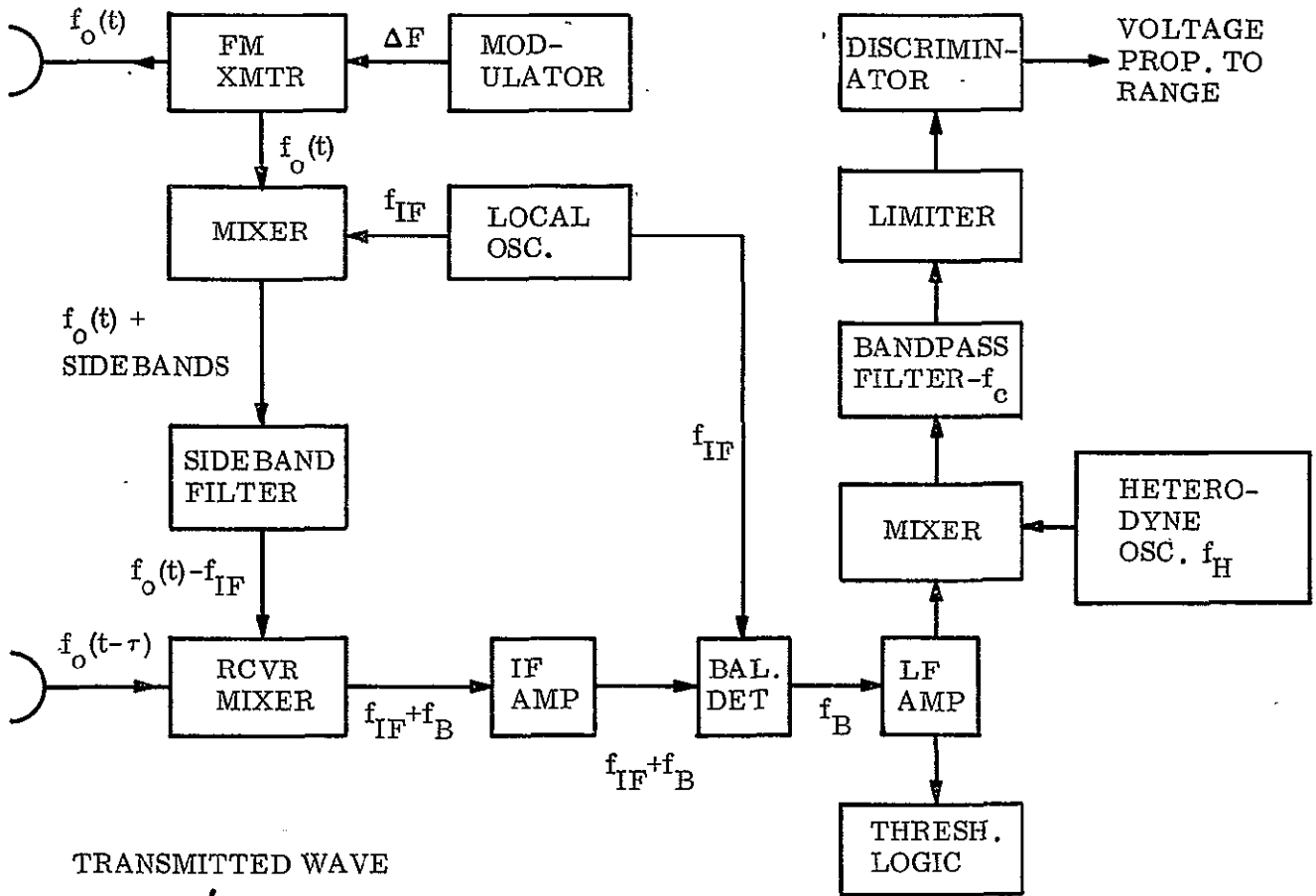
$$\delta R = \frac{246}{\Delta f}$$

where δR is in feet and Δf is in mhz. For example, for $\Delta f = 135$ mhz, then $\delta R = 1.82$ feet (.555 meters).

This fixed step error is too large, particularly in the detection of slopes. For example, for the detection of a positive slope of 35°, a range decrease of only 0.582 meters is sensed over an interval of travel of 1.0 meters, (Appendix A-1). It is thus evident that the fixed step error would have to be significantly reduced. It can be seen in the Appendix (Section A-3) that in order to avoid too many false alarms it is desirable to keep the overall RMS error of the system (this includes terrain, roll, pitch, and radar errors) down to the order of 0.1 meter if possible. Thus, the radar is budgeted to an RMS error of .053 meters. It can be seen, therefore, that even if terrain averaging were relied on to reduce the fixed step error by one half (Reference 4), the fixed step error would still have to be no more than 0.1 meters, and Δf would have to be at least 740 mhz. This value and its associated linearity requirements, is probably beyond reach with present day solid state devices (though easily achievable with backward wave oscillators). Therefore, the use of a

non-counting (continuous) frequency meter such as a frequency discriminator must be examined. The discriminator output is a voltage proportional to frequency and is continuous rather than discrete. Discriminator circuits have not been popular in the past, in FM altimeter systems, since stability and linearity problems have been experienced, particularly over a wide range of frequency operation (Reference 3).

However, discriminator circuits would be appropriate in this application. The slant range coverage will only be from about 2.75 meters to 7.0 meters or a beat frequency ratio of about 2.5 to 1. This is very small compared to the beat frequency ratios normally used in altimeters. In addition, only the slant range in the region from 3.25 meters to 5.25 meters, or a frequency ratio of 1.61 to 1, will require extra care with regards to linearity and stability. Thus, the discriminator response must be particularly linear and stable only over a 1.61 to 1 beat frequency ratio. The beat frequencies would be transposed to a higher center frequency so as to substantially decrease the bandwidth requirements. Typically, a very stable 35 khz oscillator would be chosen and heterodyned with the beat frequency which is in the range of about 1 to 2.5 khz (see Figure 5). The output of the low frequency amplifier would be heterodyned with the 35 khz oscillator and the output fed into a band pass filter. This filter will pass only the upper sidebands, 36 to 37.5 khz, and reject the lower sidebands 34 to 32.5 khz by at least 20 db. The band pass filter output would be fed to a limiter whose output goes to the discriminator. The discriminator may consist of a three pole Butterworth filter centered at 35 khz and having a bandpass of 34 to 36 khz. 36 khz, representing the 1 khz beat frequency (slant range of 2.75 meters) will be the 3 db down point of the filter, and 37.5 khz, representing the 2.5 khz beat frequency (slant range of 7.0 meters) will be 14.6 db down on the skirt (see Reference 5). The slant range of 3.25 meters will represent about 3.8 db down on the filter skirt and the slant range of 5.25 meters will represent about 9.8 db down on the skirt. Over this range, the filter response vs frequency is extremely linear, representing less than 0.2 db (< 2%) excursion from linearity. The output from the discriminator will be in volts, representing the slant range. It is, of course, evident that amplitude and frequency stability will be very essential. A self-test mode is provided whereby a calibration frequency is fed into the discriminator through the limiter to check its output voltage. This voltage should remain constant (or be compensated for) within 1 to 2% at the calibration frequency. The output of the limiter will have to be constant to within about 0.3 db or 3% over the range of voltage amplitudes fed into it. Both the IF and LF amplifiers will require good automatic gain control to minimize the range of voltage amplitude fed into the limiter.



TYPICAL VALUES

f_o	=	25 ghz
f_{IF}	=	30 mhz
ΔF	=	135 mhz
IF amp BW	=	0.5 mhz
f_m	=	200 hz
f_H	=	35 khz
f_c	=	36.75 khz

Figure 5. FM-CW Radar Block Diagram

The use of a frequency discriminator offers one mechanization technique that could be used in FM-CW systems that would eliminate cycle counting for frequency measurement. The use of techniques of this type would eliminate the inherent fixed step error and would make budgeting of a radar RMS error of .053 meters plausible in an FM-CW system.

5.1.6.2 The Ultra Short Pulse Candidate System

This system is a pulsed radar system using extremely narrow pulse widths. Time delay of the pulse return is a measure of target range. For example, a target at a 1 meter range represents a 6.6 nanosecond time delay. As was mentioned in the previous section, it is necessary that the RMS range error be less than .053 meters. Thus, time delay should be measured to an accuracy better than .35 nanoseconds. Therefore, if a 3 nanosecond pulse width is used, its time delay measurement must be accurate to better than 12% of the pulse width.

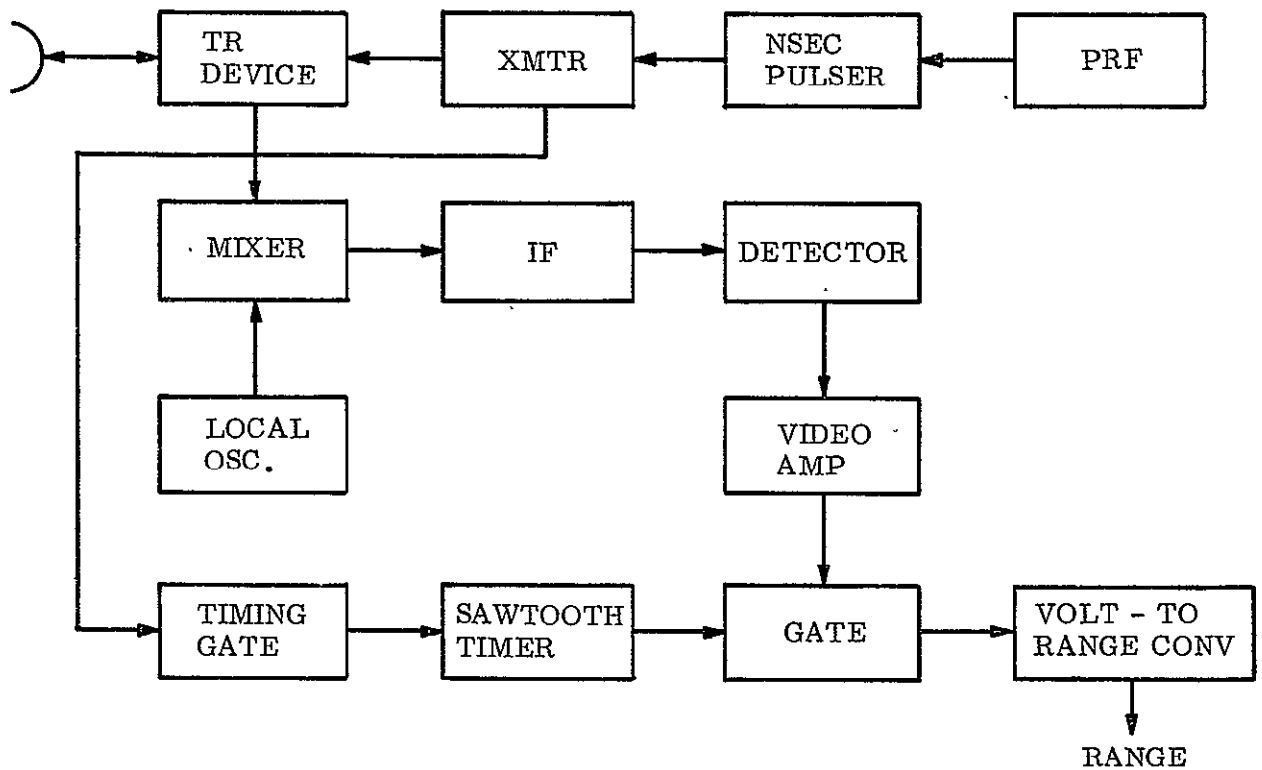
Figure 6 gives a diagram of a simplified pulse radar. For reference, some typical electrical values are: Transmitted frequency = 25 ghz; pulsewidth = 3 nanosec.; IF = 1500 mhz; IF bandwidth = 330 mhz; local osc. = 23.5 ghz; receiver sensitivity (MDS) = -75 dbm; receiver noise figure = 12 db. For comparison purposes with the FM-CW radar, the pulse radar requires a transmitted peak power of 315 MW to obtain a S/N ratio of 18 db per pulse.

5.1.6.3 The Pulse Leading Edge System

This system measures range by tracking the leading edge of the return pulse. That is, it measures the range to the closest part of the particular hazard.

Short pulses are required. However, since the leading edge is tracked, the pulse width need not be quite as narrow as for the previous case. Pulsewidths of 10 nanoseconds should be sufficient, but the leading edge rise time should be no more than 0.35 nanoseconds. The r.f. peak power requirements for this radar will be a little less than for the ultra short pulse system due to the fact that the minimum bandwidth requirements are a bit less. The block diagram of the leading edge tracker is essentially the same as for the ultra short pulse radar, figure 6, with minor modifications. The leading edge tracker will probably require both a transmit and receive antenna due to the increased pulse width.

Thus, referring to Figure 6, the TR device will be eliminated and the transmitter will be connected directly to the transmit antenna, while a receive antenna will be connected to the mixer. The gating, timer, and threshold circuitry will be optimized to respond to the leading edge of the return pulse.



TYPICAL VALUES

XMTR FREQ	=	25 ghz
PULSE WIDTH	=	3 NANOSEC.
LOCAL OSC	=	23.5 ghz
PRF	=	1 mhz
IF FREQ	=	1500 mhz
IF BW	=	330 mhz

Figure 6. Simplified Pulse Radar Block Diagram

5.1.6.4 The Ultra Short System Using Range Gating

This system employs a pulse system, uses a broader beamwidth in elevation (to illuminate more of the terrain in the longitudinal direction) and measures range by range gating the receiver. For example, using an elevation beamwidth, θ , of about 18° , (the beam may be shaped, to give a $\csc \phi \sqrt{\cot \phi}$ return so that each range cell on the ground will provide equal returns) and a depression angle, ϕ , of approximately 40° , a distance of about 2.3 meters on the ground, would be illuminated longitudinally, starting at a distance of about 1.3 meters preceding the wheelfront, and ending at a distance of 3.6 meters from the wheelfront. This longitudinal length may then be divided into five range cells by using five receiver range gates. Returns from each particular cell will in turn be sampled. Detector thresholds (which may be varied, depending on terrain type, pitch, roll, etc.) will be established for each range cell, based upon expected return from flat terrain. A strong return in a particular gate would then indicate a positive obstacle at that range, while a normal return in a particular range cell would indicate normal terrain at that range. A weak return would indicate a negative obstacle at that particular range. Since the slant range to the point that is 3.6 meters in front of the vehicle is 1.76 meters (11.6 nanoseconds) longer than that to the point 1.3 meters in front of the wheelfront, each range gate may be about 2.3 nanoseconds in width. The block diagram of the ultra short pulse radar, Figure 6, may be used with some modifications.

The sawtooth timer will trigger five gates rather than one as shown, with a total time delay of 4τ between the gates. Each gate width, τ , will be 2.3 nanoseconds wide. The first gate responds only to the return from the range cell that is 1.3 meters in front of the vehicle, (assuming flat terrain), and the fifth gate responds only to signals that are delayed in time by an amount equivalent to the return from the range cell that is 3.6 meters in front of the vehicle.

The video amplifier will also feed into the gates and the five outputs from the gates will represent the returns from the five range cells. The transmitted pulse width will be 4 nanoseconds, for this case.

5.1.6.5 Comparison of Candidate Systems

The following table compares the candidate systems.

Radar System	Advantages	Disadvantages
FM-CW	<p>Relative simplicity and low power required for short range detection</p> <p>Used in majority of altimeter applications</p> <p>All-solid-state systems are within state-of-the-art</p>	<p>Elimination of inherent step error requires a stable and linear frequency discriminator</p> <p>Separate receive and transmit antennas required</p> <p>Average range to target rather than range to closest part of target is measured</p>
Ultra short pulse	<p>Its narrow pulses provide greater ranging accuracy and finer resolution</p> <p>One antenna can perform both the transmit and receive functions</p>	<p>Short pulse systems require extremely precise electronics, high voltage supplies, and larger bandwidths which result in heavier and more complex systems</p> <p>Average range to target rather than range to closest part of target is measured</p> <p>All-solid-state systems are not within the near state-of-the-art</p>
Pulse Leading Edge Tracker	<p>Range is measured to closest part of obstacle</p> <p>Technique avoids pulse stretching produced by multipath reflections</p> <p>Extremely narrow pulse widths are not required</p>	<p>Leading edge technique requires pulses with extremely sharp rise times</p> <p>Holes will not be detected if any part of beam reflects from a surface above the hole</p> <p>Separate receive and transmit antennas required</p> <p>System complexity and weight greater than FM-CW system</p> <p>All-Solid-State systems are not within the near state-of-the-art</p>

Radar System	Advantages	Disadvantages
Ultra Short Pulse Using Range Gating	<p>Range gates provide good range resolution</p> <p>Technique provides time history of terrain as vehicle advances. Thus, terrain returns are averaged.</p> <p>One antenna can perform both the transmit and receive functions.</p>	<p>Technique requires the use of a relatively broad elevation beamwidth. This can give rise to ambiguity and multi-path problems</p> <p>Complexity and weight will be at least as great as ultra short pulse system.</p>

5.1.6.6 Choice Of A Candidate System

The previous discussion has not shown any one system to be vastly superior to all others. However, the FM-CW system has been recommended, since it is basically less complex, lighter, and more naturally suited to short ranges. It is also considered to have the least development time. Proven solid-state oscillator multiplier techniques provide suitable transmitter power and modulation characteristics at 18 ghz (Ref. 6) to perform FM-CW altimetry. By increasing the fundamental frequency 4 to 5% a system operating at 25 ghz can be obtained. No well-established solid-state sources of suitable pulse power are available to support a pulse mechanization.

Before leaving the discussion on the radars it should be mentioned that G.A.C. has been supporting an in-house laboratory effort to investigate a radar to measure short ranges.

Components for a breadboard model of a very simple FM-CW radar were assembled utilizing standard test equipment. The transmitter consisted of an Alfred microwave sweeper operating at X-band. An electronic frequency counter was utilized to measure the beat frequency. Tests were conducted under controlled conditions to calibrate the beat frequency with range to target. Preliminary field tests were then initiated. The equipment was assembled on a mobile cart and antennas mounted so that the slant range to the level ground intercept point was approximately four and one half feet. The tests were conducted in an open field utilizing a ditch two feet wide by two feet deep as a target. As the equipment was moved slowly toward the ditch a discrete change in slant range from four and one half to six and one half feet, as denoted by the frequency counter, was detected when the beam entered the ditch. These encouraging results showed the feasibility of detecting targets of concern at short ranges with FM-CW radar.

5.1.7 Power and Weight Estimates for Proposed System

Power and weight estimates have been based on some proposed and existing radar systems operating in K_u and K_a band. Estimates given by vendors of conversion efficiency (DC to RF) have varied from 0.7% (FM-CW altimeter operating at K band - Reference 6) to 0.18% for the overall efficiency of the LM landing radar. Using, therefore, 0.2% as a conservative estimate for the efficiency, the DC input power requirement would be 5 watts, based on 10 MW of RF output power. Adding to this, the bias power requirements of the twelve switching diodes, which is estimated to be of the order of 1 watt, the overall input requirement would be less than 6 watts. Weight estimates given by some vendors have varied from 1.2 lbs for a K_u band aircraft altimeter to 4 lbs for a Doppler radar operating in K_a band.

Conservatively, using 4 lbs. for the weight of the radar, plus 2 lbs for the weight of twelve antennas, and another 1.5 lbs for the support of the antennas, brings the total weight to about 7.5 lbs. The volume is estimated to be less than 100 cubic inches.

6 - SUB-SURFACE HAZARD DETECTION

The detection of voids beneath the lunar surface is important where the roof of the void is too thin to support the weight of the LRV.

Seismometry provides a technique of detecting voids with a reasonable false alarm rate and acceptable weight, cost and electrical power demand. A number of seismic methods are used on earth for various geophysical purposes. Probably the best known and most easily understood methods are those using passive instruments to detect seismic disturbances generated external to the system. The classical use of these methods is detecting distant earthquakes. More recent uses include detection of nuclear explosions and intruders (ranging from foot steps to heavy vehicles). However, since the voids that the LRV is to avoid are believed to be quiescent, active seismic methods are necessary.

Active seismometry involves a source of seismic energy and one or more sensors. In normal geophysical use explosives are used as seismic sources and geophones are used as sensors, converting the received seismic energy to electronic signals that can be amplified, processed and displayed (Ref. 7). Typically, a string of geophones is buried (or at least the spikes driven into the ground) along a straight line. The explosive is buried at some distance beyond one end of the line, see Figure 7. Where the successively deeper rock formations have increasing seismic velocities, significant amounts of energy will be refracted to travel along each of the discontinuities. The depth to each discontinuity can be determined by measuring the arrival times at each of the geophones. If, in such a geologic structure a void existed along one of the discontinuities, as shown in Figure 8, several different phenomena could be used to detect it. These include an additional delay, increased attenuation and oscillation or ringing of the walls of the void. The refraction configuration has the disadvantage of such a widespread of geophones and source as to be impracticable from a moving vehicle. Closer spacing of source and geophones is used occasionally for reflection seismic shots, as shown in Figure 9. Presence of a void, as shown in Figure 10, could be detected on the basis of an additional reflection, shadowing of known reflections (from deeper layers) (Ref. 8) by increased delay or attenuation, and oscillation of the walls of the void.

While all of the phenomena mentioned above have been used to detect the presence of subterranean voids, each has its own advantages, disadvantages and limitations (Ref. 7, 9, 10, 11, 12). All phenomena unique to refraction techniques are impracticable for use with the LRV due to the spacing between source and geophones being much larger than the vehicle.

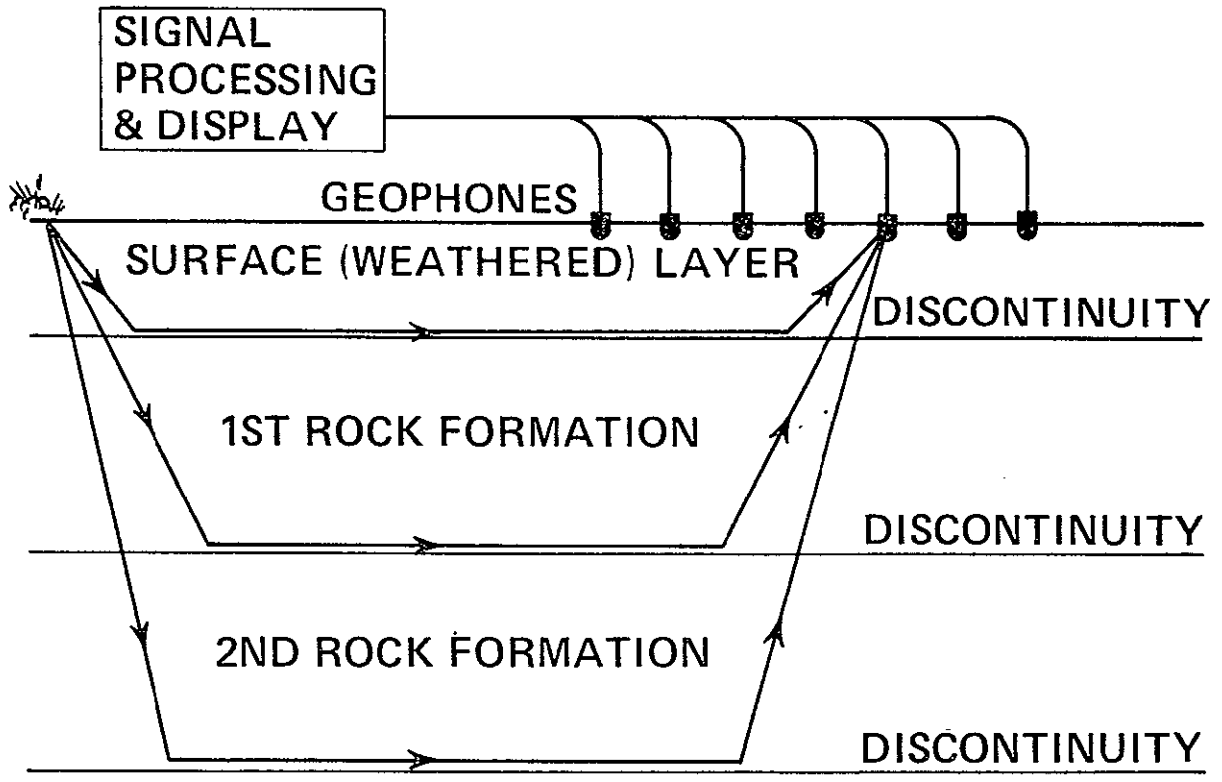


Figure 7. Seismic Refraction Shot

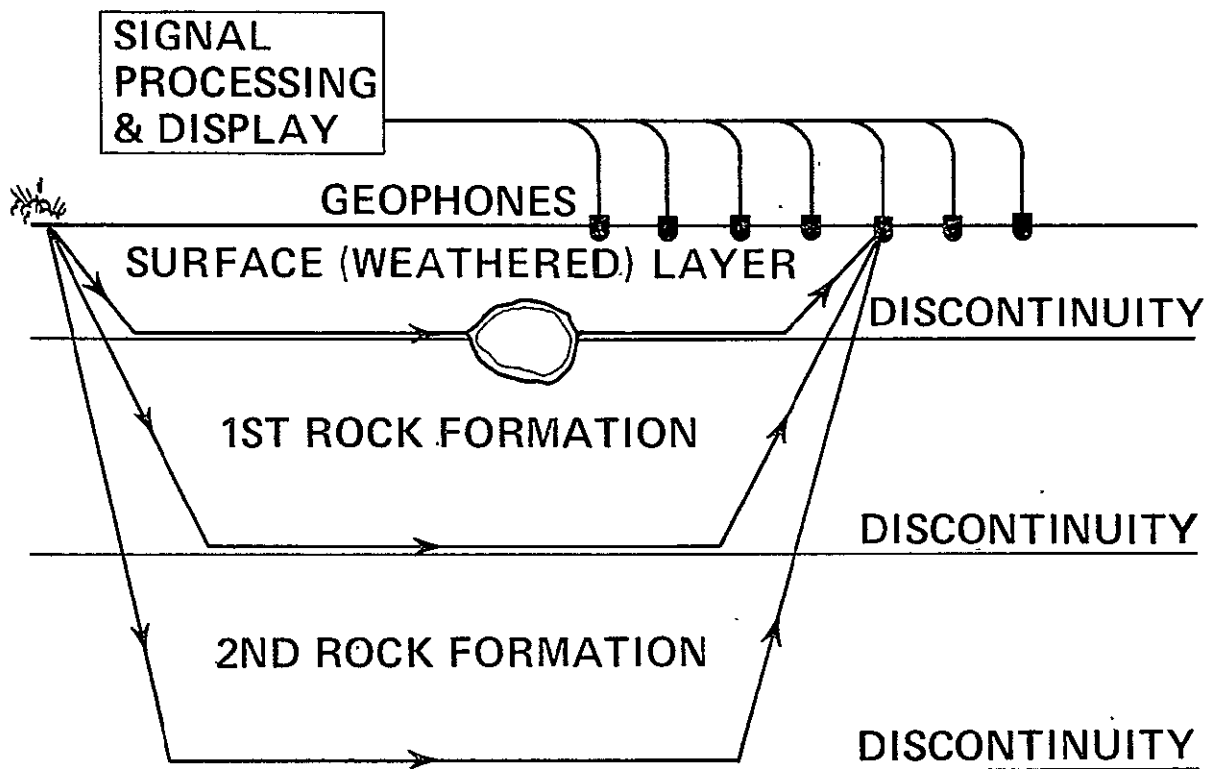


Figure 8. Seismic Refraction Shot

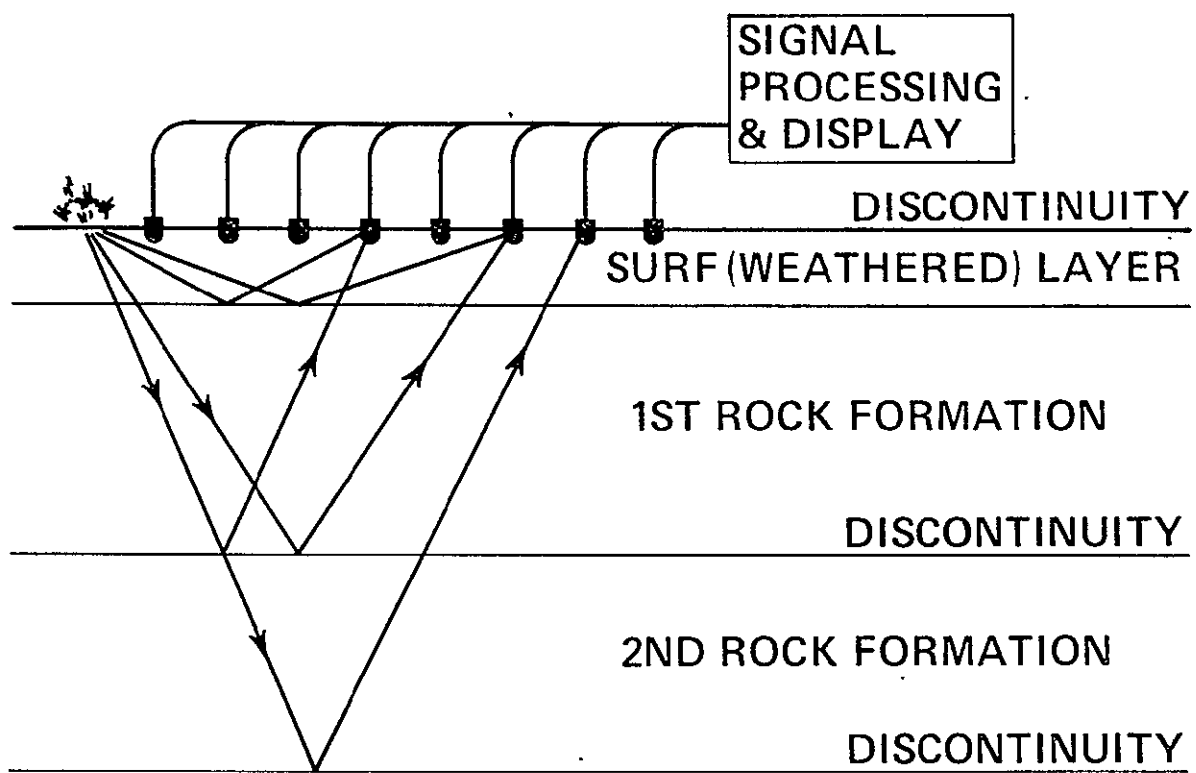


Figure 9. Seismic Reflection Shot

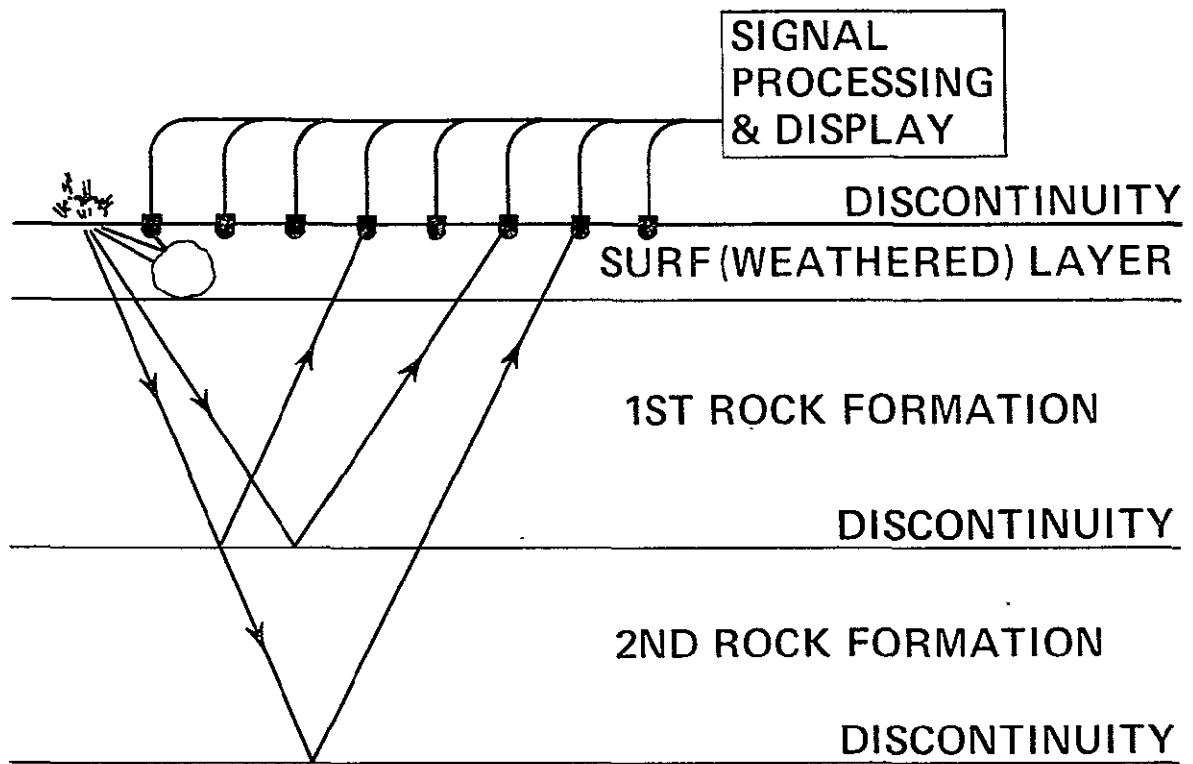


Figure 10. Seismic Reflection Shot

To be practicable, all elements of any system should be within, or at least fairly near, the perimeter of the vehicle. Increases in delay and attenuation can be caused by many different geological structures in addition to the voids that could be hazardous to the LRV. Such geological structures as thin cracks (of the order of a centimeter wide) and interfaces between different types of rock and materials can include numerous interfaces similar to shale. These discontinuities can also return echoes in a reflection configuration. These geological formations can also cause shadowing of known echoes. On the other hand, oscillations of the walls of a void are only known or expected in large voids of the type that are expected on the moon (Ref. 13). All other phenomena that have been tried on earth suffer from many signals similar to those from voids resulting in a poor signal-to-noise ratio and hence causing a poor probability-of-detection and/or an excessive false-alarm rate (Ref. 14). Thus, the use of a system designed to detect oscillations of the walls of a void should provide a significantly higher probability-of-detection and/or lower false-alarm rate than any other known seismic type of system.

The significant difference between the voids that cause oscillations and the formations that do not is shape. The lava tubes that Watkins (Ref. 13) found to oscillate had cross sections that were approximately circular, while the geological structures that pose no hazard to the LRV tend to be characterized as thin cracks. However, the significant difference is not in the curvature or height-to-width ratio. It is rather the structural continuity all the way around the perimeter of the void cross section that appears to be important. Thus with a circular cross section, a perturbation can travel all the way around the circumference without significant losses. Cracks, however, tend to extend for relatively great distances without a marked end. In addition, where the two sides do join, they are so close to being parallel that very little energy can reverse direction to travel around the crack. Most limestone caves on earth were originally started by water seeping into stress cracks. These cracks usually extend well beyond the cave in both directions. Thus, even if this type of cave has a circular cross section, cracks extending out radially will attenuate or block wall vibrations that would otherwise travel all the way around.

The lava tube from which Watkins first observed the wall oscillations had a cross section that was not at all circular. It was quite irregular in shape, with the width-to-height ratios averaging around four to one (Ref. 13). Watkins extracted from a more theoretical paper by Biot (Ref. 15) the following equation for diameter of the lava tube (D) as a function of shear velocity (V_s) of the rock it is in and the frequency (f) of the oscillations:

$$D = \frac{V_s}{1.55 f}$$

Rearranging, frequency can be computed as a function of diameter and shear velocity.

$$f = \frac{V_s}{1.55 D.}$$

However, the original equations all assumed a circular cross section. In this case, the actual circumference (C) can be used in lieu of the diameter:

$$\begin{aligned} C &= \pi D \\ D &= C/\pi \\ f &= 2.2 \frac{V_s}{C.} \end{aligned}$$

Unfortunately, however, some of Watkins field results gave frequencies as much as three times as high as indicated. This was considered due to failure to meet Biot's original assumptions of a circular bore in an infinite solid. In each case the ceiling of the cavity was close to the surface. Roof thickness was less than the effective diameter. The validity of the equations appear questionable, but they still provide the best available method to estimate frequency as of this writing. If the smallest void of concern is one meter in diameter and shear velocity is estimated at 1,000 meters per second (higher than any found by Watkins), a maximum expected frequency of about 650 Hertz is computed. Allowing for three times that (to be compatible with Watkins) gives an upper frequency of about 2 Kilohertz. Thus, it is desirable that the ability to receive and process narrow band signals at least up to 2 Kilohertz be provided at least in the first operations on the moon.

So long as the voids of hazardous dimensions on the moon are similar to lava tubes, oscillations should be the best means of detection. This is predicated on a volcanic history of the moon that included the production of lava tubes, and not including any other voids that might be hazardous to the LRV (but are incapable of oscillating). This ideal situation, all hazardous voids being of the most easily detected type, can only be confirmed with extensive tests on the surface of the moon. First the existence of any voids of significant size must be established. Second, the oscillations must be determined. Last, the lack of all other voids must be established over a statistically significant area of the moon. The last step comes down to traversing large distances on the moon using detection of seismically induced oscillations to avoid lava tubes. If the vehicle does not fall into any

voids, the moon can be assumed free of them (at least tentatively assumed). As crude as this approach appears, it is probably the only alternative to instrumenting the LRV seismic hazard detection system to detect both oscillating and non-oscillating voids.

The data announced so far from the seismic shock generated by crashing the lunar module from Apollo 12 into the moon has been quite interesting, but of little significance to the short range seismics intended to be used with the LRV to detect hazardous voids. The time periods involved imply transmission over distances and depths vastly greater than those needed to detect hazardous voids. However, it would be very helpful if the signals received from that shock could be analyzed for oscillations or individual frequency components. If there are voids of the type that can oscillate in significant numbers on the moon, the oscillations should have been present in the seismic signals transmitted to earth. However, seismologists do not usually look for this type of signal. In addition, it is quite possible that due to the nature of the impulsive signal and the multiple paths, probably with many reflections, there was a high level of broad band noise that obscured the void wall oscillations.

Detection of oscillating voids could possibly be accomplished with a relatively broadband detector, 10 to 2,000 Hertz, for instance (Ref. 13). Data from previous seismic tests on the moon would be used to make final determination of the frequency band of interest. The upper limit could eventually be reduced when the relationship between void size and frequency for the lunar surface material is established. Voids less than one meter in diameter will oscillate above the optimum upper corner frequency. Lower corner frequency will be determined by the largest void detected.

If the signal-to-noise ratio is not good enough for reliable detection with a reasonable false-alarm-rate it can be improved by applying signal processing techniques. The most likely approach is reduction of bandwidth. With narrower bandwidths less noise and undesired signals can reach the detector. The optimum processor gain can be achieved by narrowing the bandwidth to that of the signal. Watkins (Ref. 13) reports that the oscillations lasted about one second, implying a bandwidth of approximately one Hertz. Thus, by using a detector bandwidth of one Hertz, it will be just wide enough to pass the oscillation from the void, but not wide enough to pass any more noise than is necessary. The narrow bandwidth detector, however, is not without disadvantages: a time constant that is relatively long (one second in this case) and coverage of only the one narrow band, unless the complexity of a bank of comb filters or a frequency sweeping system is incorporated into the system. It is possible that a compromise bandwidth between ten and one hundred Hertz would provide

adequate signal processing gain while keeping the cost, weight and power consumption to a minimum. However, the decisions on effective processing bandwidth, upper and lower frequency limits of the band to be processed and type of processing cannot be made until more data from the moon becomes available. Of prime importance are the frequencies and the signal-to-noise ratios likely to be received.

Detection of non-oscillating voids would (if desired or needed) call for wide band detection. Knowledge of the propagation losses as a function of frequency and the frequency characteristics of any echoes would be helpful, however, most systems of this type have broad frequency responses with little or no criticality regarding optimum values. Since short ranges are involved and good resolution is desired (but not vital), higher than usual seismic frequencies appear desirable. It would appear that inclusion of a broad band detector would provide little additional complication compared to the signal processing that will probably be required for optimum detection of oscillating voids. However, the false alarms that appear likely from a broad band detector might very well limit its usefulness.

All of the preceding discussion has been aimed at merely detecting the presence of hazardous voids. Localization, however, is also important so that intelligent decisions can be made to avoid traveling over the void. The prime requirement in this case is to be able to measure whether the void is to the right or left of the vehicle and approximately at what angle. By providing two geophones, one along the right side of the vehicle and one along the left, directional information can be derived. Measurement of relative arrival times at the two geophones will provide the required information. It should be noted, however, that the use of arrival times at right and left geophones will not tell whether a given signal is in front of or behind the LRV. It can be presumed that as the LRV traverses the lunar surface all newly detected voids are initially in front. However, sharp maneuvers such as tight turns or backing could complicate decision making. If four geophones were used, right and left in front, and, right and left behind, relative arrival times will provide enough information to define the spherical angle to the void. Further study is needed, however, to determine whether the extra expense, weight and power consumption are justified.

6-1. SEISMIC SYSTEM

As has been indicated earlier in this section, merely finding a usable seismic phenomenon is not sufficient. A practicable method of generating seismic signals, inserting them into the lunar surface and receiving the returning signals is required. Normal seismic practice is to bury the explosive charges from 0.1 to 1 meter or more below the surface.

Spikes integral with standard geophones are driven into the surface to provide seismic coupling. After the required shots the geophones are pulled from the ground and retrieved for use on future shots. All of these steps make use with the LRV, which must continue moving without unnecessary stops, impracticable. The goal of this study was to investigate techniques that would provide seismic detection of hazardous voids while the vehicle moved continuously. The only acceptable reasons for causing the LRV to stop is to avoid traveling over a void, or, on rare occasion, to wait while a marginal suspicious signal is transmitted to earth for analysis and decision.

The initial problem is to provide some means of coupling between the transducers and the lunar surface in a manner that does not interfere with forward motion of the LRV. The simplest approach appears to be mounting a number of transducers around the circumference of one or more wheels so that one or more sources and geophones are always in contact with the lunar surface. Most designs include wheels that have a relatively large segment that is flattened where it is in contact with the surface. Thus, by placing a reasonable number of units around the tread of a wheel, at least one will always be in contact with the ground. Other methods were considered briefly, such as multiple arms that would place individual sensors on the lunar surface, hold them in place as the vehicle moved forward, then lift and move forward to the next location. This was considered to have complexity power and control requirements that placed it well beyond the physical constraints of the LRV. If longer periods of time in contact with the lunar surface were judged necessary a system utilizing a belt of chain rolling over two wheels, keeping the transducers in contact with the ground, could be considered.

Most mechanical devices tend to be noisy. Latching vibrations and similar functions of the seismic source could easily interfere with geophone operation between intended seismic pulses if both source and geophone are mounted on the same wheel. In addition, the seismic impulse could easily reverberate through the structure of the wheel; around and around the circumference and back and forth along the spokes. In either case the reverberations from within the wheel could easily continue long enough to mask returns from voids. Therefore, it is quite desirable to use separate wheels for the seismic sources and the geophones. In addition to keeping the noise and reverberations of the sources away from the sensor wheel and the geophones on it, the noises due to crunching under the vehicle weight and due to slippage should also be avoided if optimum detection is to be achieved. Thus the sensor wheels should be separate from the main LRV wheels that carry the vehicle weight and are used for propulsion. A possible configuration places the sensor wheels out in front of the vehicle so that it will be closer to the voids, providing detection at greater

ranges in front of the load bearing wheels (that could break through the weak roof of a void). The sensor wheels could also be placed along the side of the vehicle, either between the front and back drive wheels or outboard of the drive wheels on each side. If field tests show that these configurations provide a signal-to-noise ratio significantly better than necessary, then it would be worth while to try mounting the geophones on the front wheels and the sources on the rear wheels. Due to the shock associated with the impact of the seismic source it is desirable that the wheel with the sources carry enough weight that the source can remain in contact with the lunar surface during all portions of the seismic pulse. Noise due to weight and slippage is no problem on the source wheel. Therefore, it is perfectly permissible to mount the seismic sources on one (or more) of the regular LRV wheels.

6.2 SEISMIC SOURCE

In typical seismic practice explosive charges are used as the source. However, they have several serious drawbacks when used with the LRV. As expendables used at short distance intervals, a large number would be required. If one were used every ten meters of travel, a quantity of 100,000 charges would be needed for a 1,000 kilometer trip. Safety requires special handling of explosives. In the required quantities the potential danger is extreme should there be an accidental firing. On the other hand, the use of mechanical sources eliminates these problems. Two different types of sources are proposed, one operated by gravity, the other by compression of a spring.

The gravity powered hammer seismic source wheel is shown in Figure 11. Three spoke-like tubes are mounted within the wheel. Almost any number could be used, but three will be assumed until field tests indicate how many seismic pulses are needed for each full turn of the wheel. Within each spoke is a steel ball that falls back and forth from one end to the other as the wheel turns, acting as a hammer. When it strikes the anvil at the bottom end the shock is transferred to the lunar surface, on which it is resting. A permanent magnet next to the anvil holds the hammer in place as the wheel rotates, moving the hammer up to the top. When it reaches the top (position 1 in Figure 11), a pulse of current through the release coil momentarily cancels the field of the holding magnet, permitting the hammer to fall down through the tube (position 2) striking the anvil (position 3). Each hammer in each of the other tubes operates in the same way. Each hammer gives two seismic impulses for each full turn of the wheel.

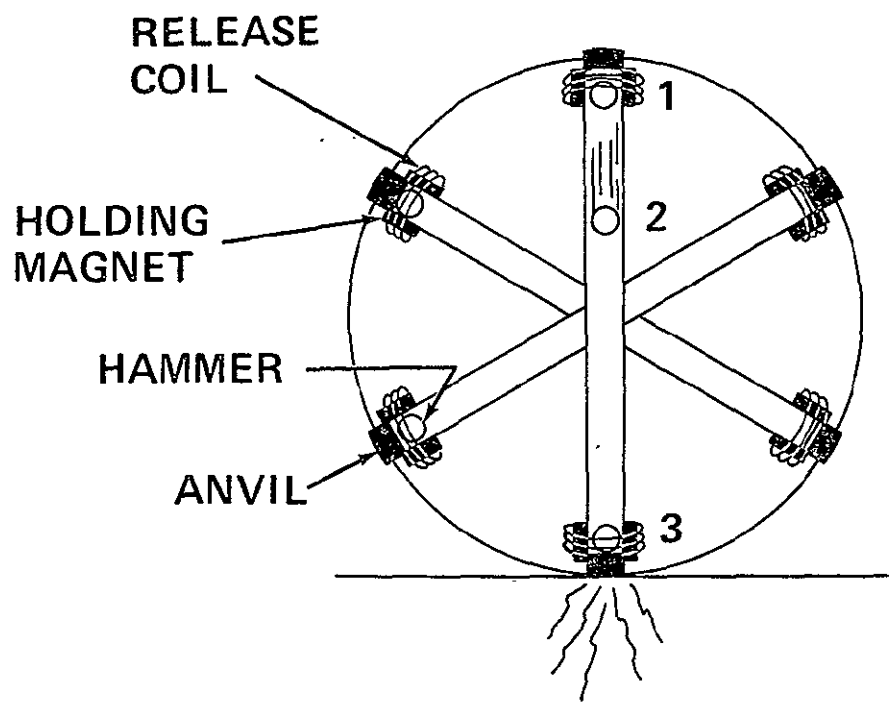


Figure 11. Gravity Hammer Rolling Seismic Source

Two possible problems could limit the desirability of the gravity hammer. First, the tubes would be relatively sensitive to damage from bending or denting. Either of these damages could slow down or stop the hammer. Secondly, the magnetic fields from the holding magnets and the release coil could interfere with the magnetic measurements planned to be taken along the moon's surface.

The alternate type of source utilizes a number of spring-loaded hammers around the circumference of the wheel, as shown in Figure 12. Details of the operation of the individual hammers are shown in Figure 13. These operate in a manner very similar to the automatic center punch used by many machinists and mechanics. While one of the spring-loaded hammers is at the upper part of the wheel, the spring and shaft are fully extended. As the wheel turns, the device is rotated down to where the shaft contacts the lunar surface. Further rotation forces the shaft in, compressing the spring. Just before the shaft is pushed in all the way, the trigger (shown inside the spring) hits the top of the barrel (center portion of Figure 13) and releases the hammer from the shaft. The spring forces the hammer down until it strikes the anvil. The impact from the anvil is transmitted to the lunar surface by the shaft. If control is desired of the triggering, a magnetic or hydraulic device can be used for this purpose. However, the flexibility achieved by controlling exactly when a given device triggers is achieved only at the cost of additional complexity and computer requirements. In any case, the spring must be damped to prevent vibrations interfering with the seismic returns from voids.

It should be noted that while the two mechanical seismic sources appear to be small, cheap and reliable, and require no large amounts of electrical power, the energy to operate them actually is taken from the propulsion motors. The raising of the gravity hammer and the compression of the spring each require additional power from the propulsion motors. The exact amount of energy required will depend upon their final configuration on the vehicle.

6.3 CONFIGURATION ON VEHICLE

One possible configuration is shown in Figure 14. Mechanical sources (spring loaded hammers) are mounted on both front propulsion wheels of the LRV. The redundancy is provided only for back up. Control is provided only to allow all hammers on one side or the other to operate. The geophones are mounted on two sensor wheels pushed ahead of the LRV. The use of two sensor wheels provides redundancy in case of failure on either side or seismic anomalies that attenuate the signal to one side. In normal operation measurement

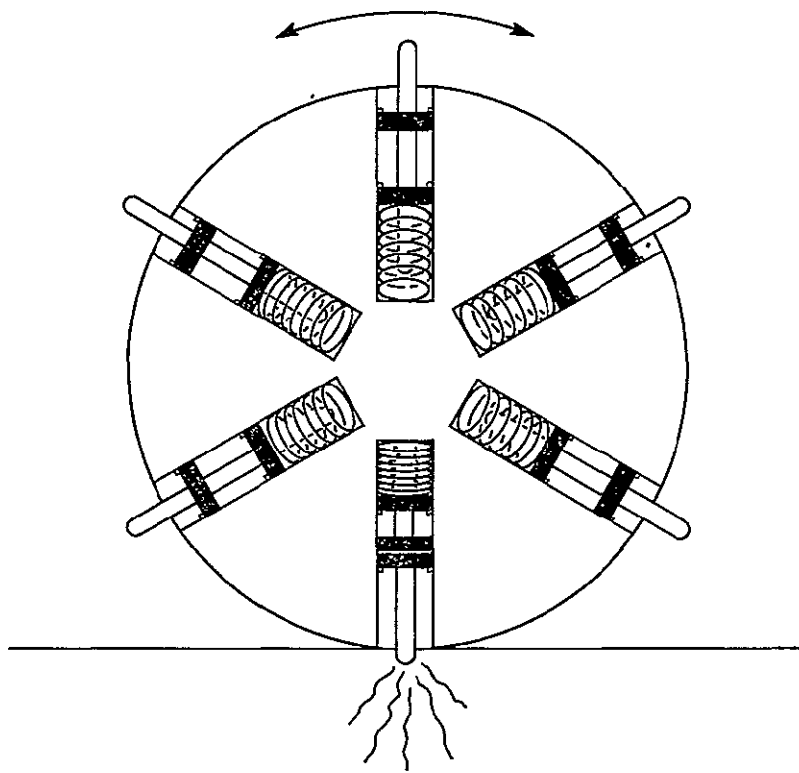


Figure 12. Spring-Loaded-Hammer Rolling Seismic Source

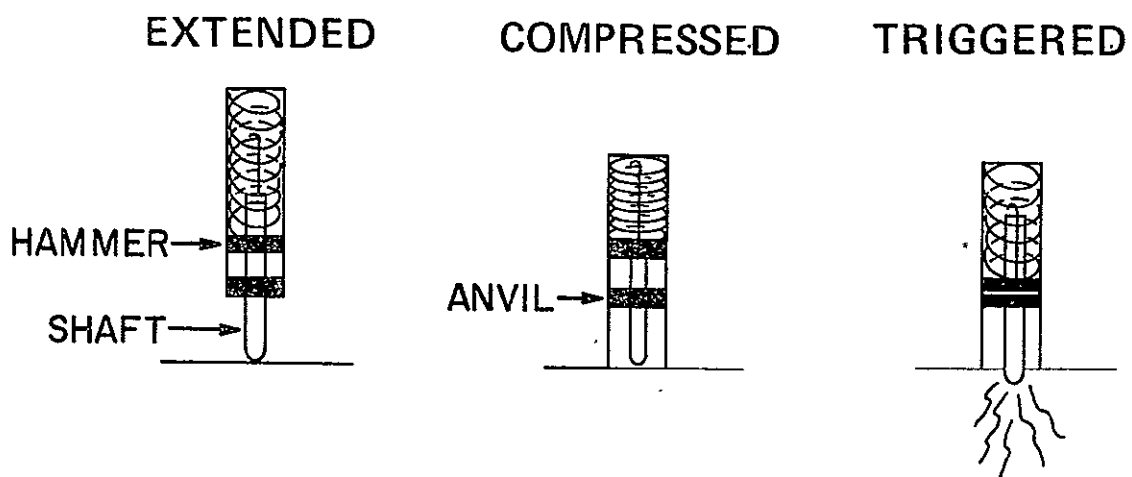


Figure 13. Spring-Loaded-Hammer Seismic Source

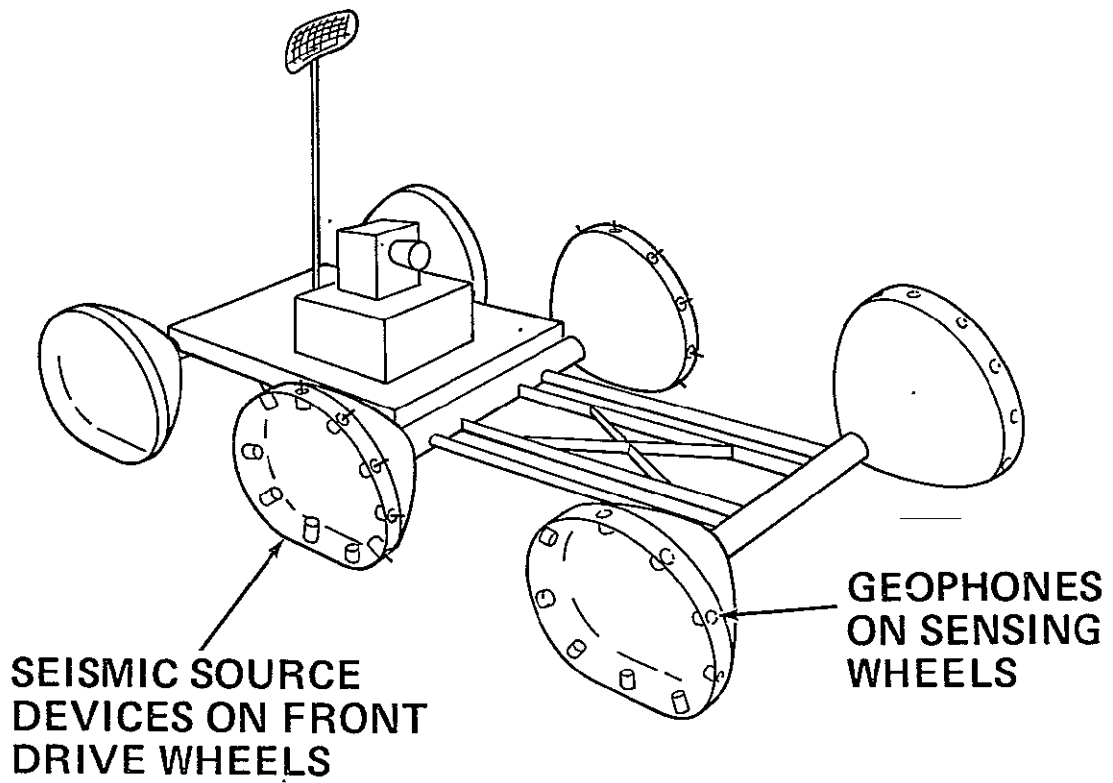


Figure 14. Seismic Void Detectors on LRV

of the time difference between arrivals at the geophones on the two wheels provides information as to angle of each void with respect to the direction in which it is headed. In addition to relative time measurement, signals from each of the sensor wheels is analyzed both for narrow band responses (oscillations) and wide band ones. For difficult decisions the vehicle stops and sends the questionable signals to earth for detailed analysis and orders for the next move.

6.4 SOIL PENETRATING RADAR

The detection of sub-surface hazards to the LRV may be feasible with the use of soil penetrating radar. The present study located numerous articles in the literature published by groups investigating the earth sciences and soil trafficability in which the feasibility of utilizing RF techniques for the determination of soil parameters was analyzed. U.S. Army agencies such as the Cold Regions Research and Engineering Laboratory, (Ref. 16), and the Waterways Experiment Station (Ref. 17), have been conducting soil and ice trafficability studies utilizing remote sensors for the past decade. Numerous companies such as, Texas Instrument, Barringer Research, Adcole, Southwest Research Institute, and General Dynamics Electronics have also performed research in this area, (Ref 18, 19, 20, 21, 22).

Many techniques for measuring soil thickness were found in the literature. Two of these for which successful field tests have been reported and which offer approaches to the LRV sub-surface problem are the Barringer Research RF technique for measuring ice thickness (Ref. 20) and the General Dynamics Electronics radar technique for detecting voids beneath the surface (Ref. 21).

The first of these is a VHF Pulse Compression System called the 'chirp' method. This technique transmits a broad band signal ranging from 100 to 600 mhz into the surface. For a given layer thickness there will be a particular frequency of incident radiation for which the layer will be exactly 1/4 wavelength deep. The sub-surface reflection will then arrive 180° out of phase with the surface reflection so that cancellation occurs. The receiver contains many tuned filter circuits, and the filter circuit that corresponds to the layer's quarter wavelength thickness will contain minimum energy detectable by minima discriminator. A second sub-surface reflection indicating the bottom of the void can be obtained with this technique with the addition of an extra bank of filter circuits and discrimination logic.

The second is a time delay method. This technique transmits a short pulse approximately 2 nanoseconds long in the 300 mhz range into the surface. Theoretically three return signals will be received; one from the surface, one from the top of the void and one from the bottom of the void. By comparing the time delay between the received signals, the depth to the top of the void and the bottom of the void can be determined. In an operational model the signals are sent to a CRT where visual analysis is performed by an experienced operator, however, it is feasible that the system could be made automatic with the proper filtering and discrimination logic.

Soil penetrating radar offers an approach to detection of sub-surface hazards, however, there are numerous problems associated with its application to the LRV. The frequency which most techniques use is in the UHF-VHF range. The enormous antenna sizes associated with lower frequencies and the extremely high soil absorption loss associated with higher frequencies led to the selection of this frequency range. Even this frequency range requires antenna sizes approximately one meter square of special design to give a useable directionality to the system.

The power requirements do not appear to be excessive for LRV application. Considering a simple power equation:

$$PT = PRX + PL + PR + PS - PAT - PAR$$

where: PT = Transmitted Power
 PRX = Received Power
 PL = Two way Path Loss
 PR = Surface Reflection Loss
 PS = Soil Absorption Loss
 PAT = PAR = Antenna Gains

and using conservative values, the required transmitted power would be:

$$PT = -40 + 60 + 10 + 3 - 6 - 6 = 21 \text{ dbm}$$

or 0.126 watts.

If this transmitted power is converted to system power using a conservative value of 1.5% efficiency, an acceptable system power of 8.4 watts would be required. While all values used in the illustrative equation are considered conservative the value of 3 db selected for soil absorption loss is worth further discussion.

This value is based on a theoretical lunar soil absorption loss of 0.5 db/meter and a penetration depth of 3 meters. The attenuation may change depending upon the actual

characteristics of the lunar soil. At the VHF band and higher the attenuation is mainly dependent on the transmitted wavelength, the dielectric constant of the material and the loss tangent or dissipation factor of the material. If the three parameters are known the attenuation can be determined from the nomogram in Figure 15 (Ref. 23). The loss tangent is a non-linear function of frequency which may peak at more than one value of frequency. Dielectric constants and loss tangents of many dielectrics for various frequencies have been empirically determined and are listed in the literature (Ref. 23). Applying these values to the nomogram of Figure 15, the relationship of attenuation vs frequency for different soil types were determined and plotted in Figures 16 and 17. Figure 16 shows this relationship for soils with zero moisture content and also for vacuum dried 1/4 inch pumice which theoretically resembles lunar soil (Ref. 19). It can be noted that all the materials plotted exhibit attenuations less than 1 db/meter at 300 mhz. However, as the frequencies approach the microwave region the attenuation losses become prohibitive. The exception to this trend appears to be loamy soil. If actual lunar soil is found to exhibit similar characteristics to loamy soil then the possibility of utilizing higher frequencies and smaller antennas in this technique might be realized. However, surface roughness imposes an additional limitation in the use of higher frequencies. Taking the empirical figure of 1/10 of a wavelength as the maximum tolerable surface roughness before reflectivities become severely modified by surface texture, gives curvatures (particle diameter) of 10 cm at 300 mhz, 3 cm at 1 GHZ and 0.3 cm at 10 GHZ.

Figure 17 shows the attenuation vs frequency relationship for soils with varying degrees of moisture content. It is apparent from these plots why transmission to meaningful penetration depths in typical earth soils requires excessive amounts of power.

Another consideration in the use of soil penetrating radar is the incident angle. All reported tests were conducted at normal incidence keeping reflection losses and complexities in received signal to a minimum. It is obvious that transmission at off normal incidence would cause increased losses in reflected power but more significant is the accompanying complexity in the return wave form due to refractions at the interfaces.

A sub-surface hazard detection system restricted to present state-of-the-art techniques would require utilization of a boom which would suspend the antenna or antennas two meters in front of the vehicle allowing transmission of signals at normal incidence. Any voids detected in the beam coverage less than a threshold depth would cause a stop signal to the vehicle.

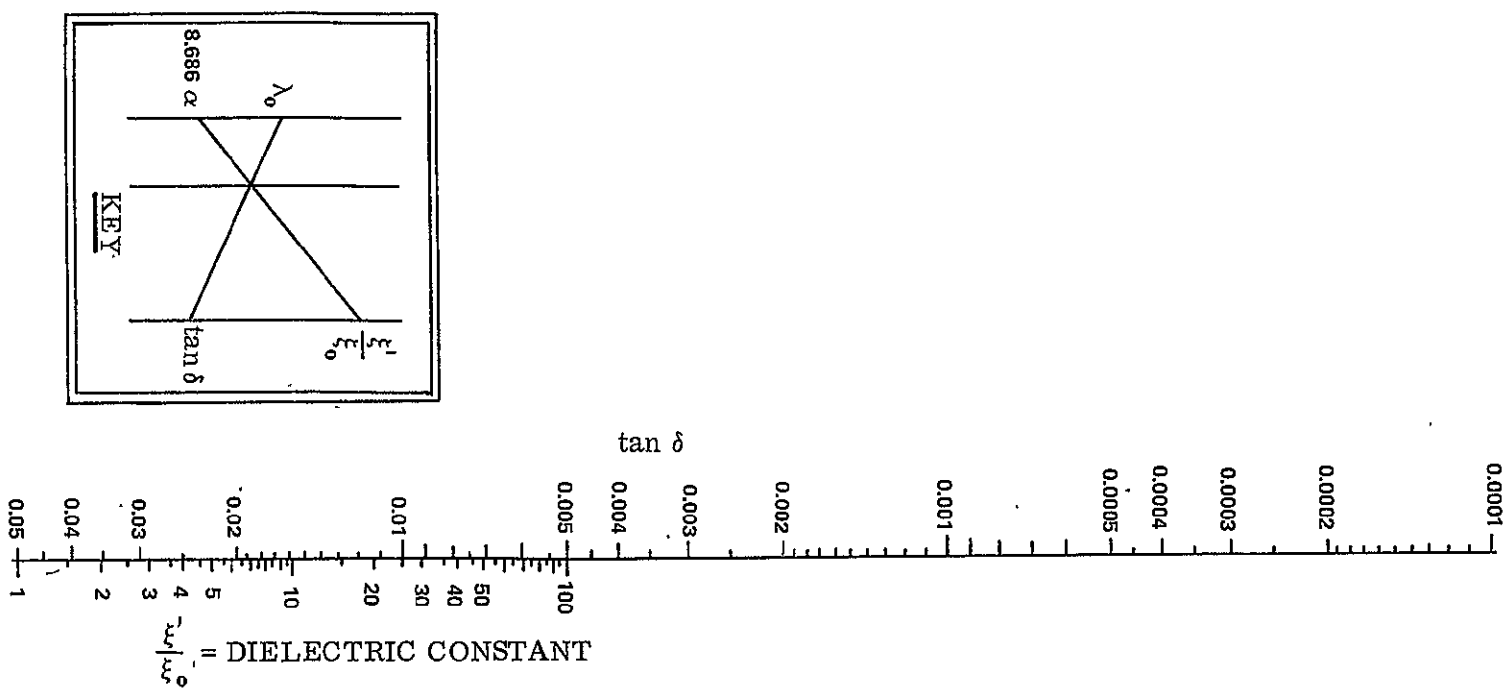
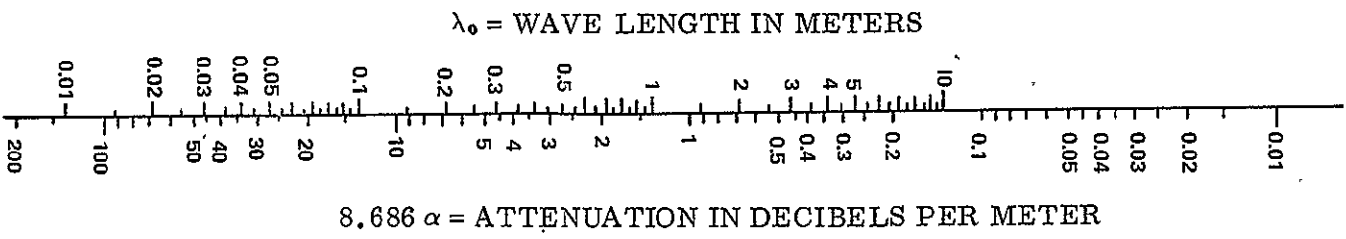
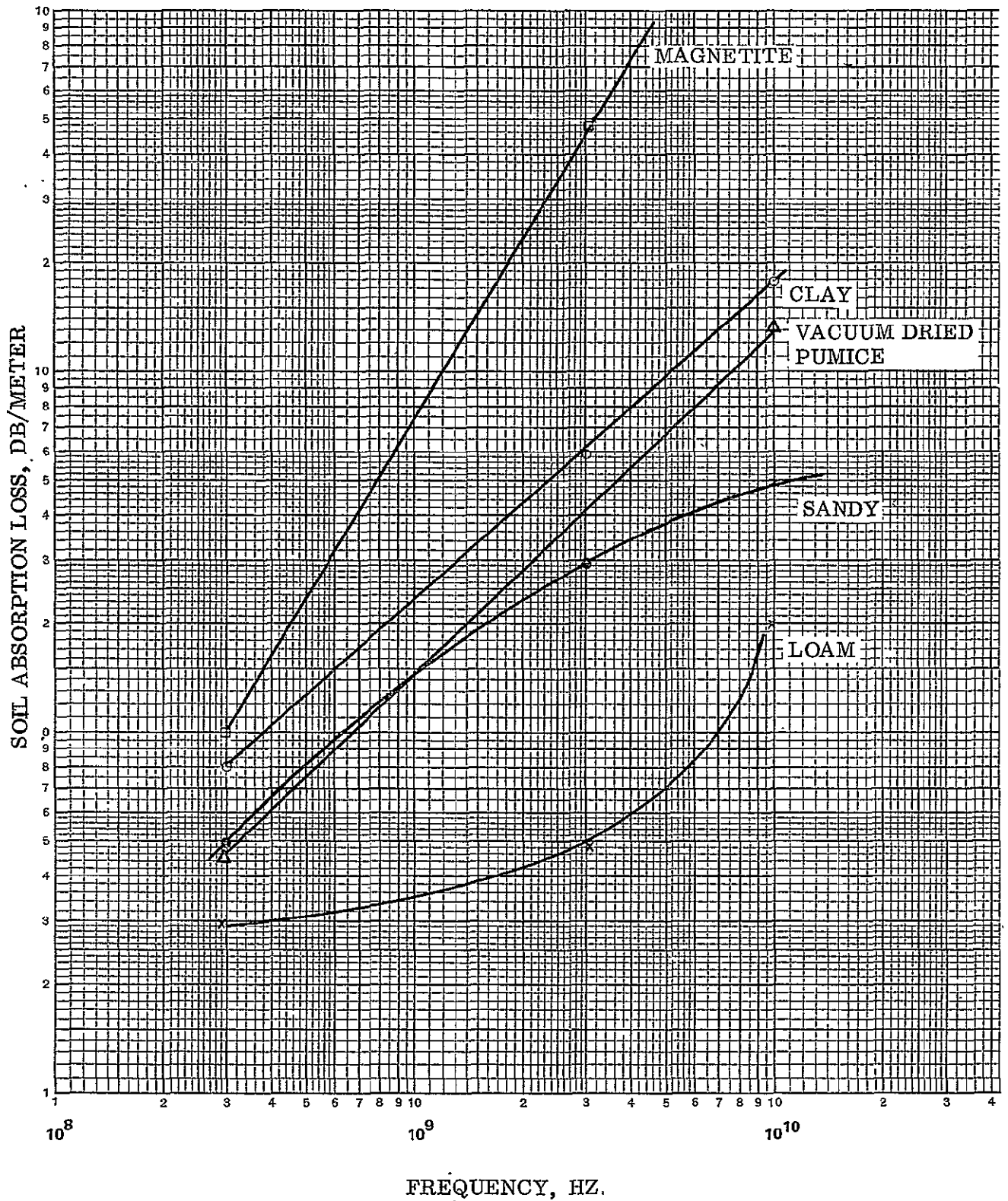
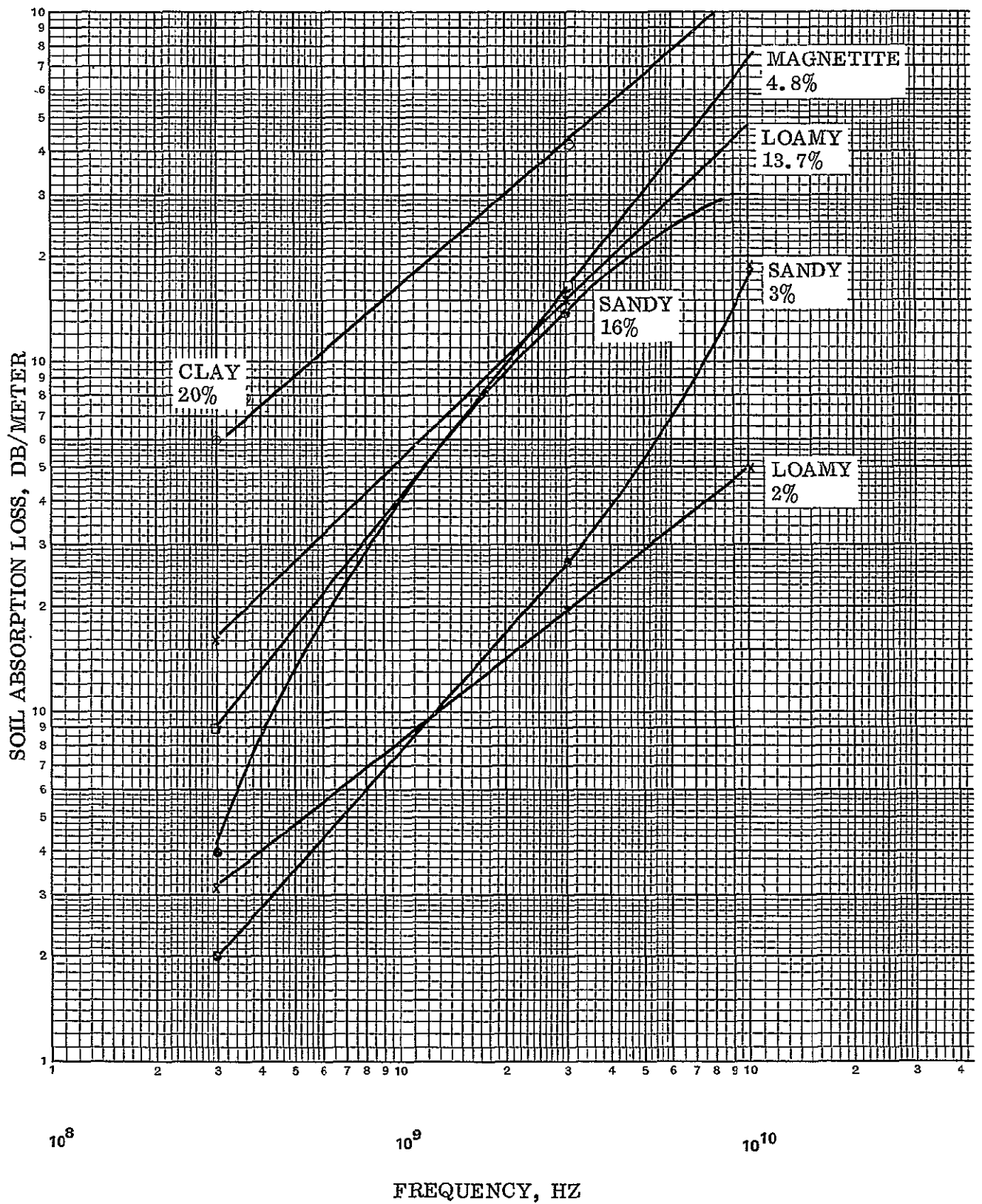


Figure 15. Decibel Loss per Meter for Low-Loss Dielectrics



1. ALL SOILS HAVE ZERO MOISTURE CONTENT
2. VACUUM DRIED PUMICE SIMULATES LUNAR SOIL

Figure 16. Soil Absorption Loss vs. Frequency



1. MOISTURE CONTENT NOTED IN PERCENT

Figure 17. Soil Absorption Loss vs. Frequency

The determination of a value which constitutes a threshold depth will depend upon the final vehicle configuration and the overburden that it presents to the lunar surface, and the actual cohesive strength of the lunar soil. Since both parameters have not been defined to the degree of accuracy required to provide a reasonable assessment of surface layer thickness that would constitute a hazard, the assignment of sub-surface hazard threshold values would be difficult until such data became available.

6.5 ADDITIONAL TECHNIQUES

A number of "state-of-the-art" geophysical exploration techniques for the detection of sub-surface voids have been proven on earth (Ref. 7). Of these methods, the least likely lunar candidate is magnetism, due to the paucity of information on the magnetic characteristics of the lunar surface and the very low level of ambient magnetic field of the moon (Ref. 24). It is apparent that the magnetic influence of the LRV, especially the drive motors, would make detection of weak signals difficult. Due to the lack of information about the magnetic structure of the moon it would be impossible to predict either the signature of a void or of other formations that might look like a void, but present no danger. (The latter signatures would be false alarms.)

Gravimetry would very likely work, but is impractical in this application. Gravity meters have been successfully used to find caves on earth (Refs. 9, 10), however, for each measurement the instrument must be placed on the ground, leveled, allowed to stabilize and then read by the operator. Since the gravity meter is on the ground, the operator must sit or lie down to level and to read it. This would have to be repeated every few meters. Obviously the operation of the gravity meter is not compatible with LRV speed or automation requirements.

Measurement of electrical resistivity offers promising possibilities. Initial tests on the first samples of lunar surface material returned by Apollo 12 indicate reasonable electrical conductivity (Ref. 25). Resistivity measurements have successfully found several previously unknown caves on earth (Refs. 11, 12). Three potential significant problems would have to be overcome before resistivity could be used for detection of voids from the LRV. First, some method of making good electrical contact with the lunar surface must be developed. This must have a large surface area of contact so that contact resistance is not too large compared with the path resistance. The contact resistance must be fairly constant, since variations will appear as noise. Secondly, the presence of the LRV must not cause a significant change in the measured resistance. Presumably it would be necessary to isolate each wheel from the others electrically. Once this has been done, the wheels can be used to make the contact for the measurements. The impact of this kind of structural change

on the LRV is not known at this writing. Lastly, more must be learned about the electrical conductivity of the rest of the lunar surface and down to greater depths. If significantly large areas have resistance anomalies, either at the surface or at shallow depths, detection of voids will be very difficult.

Radiometry has also been used on earth over voids (Ref. 26). Normally a cool spot indicates a void. Either infrared or microwave wavelengths can be used, however, this phenomenon is not well understood and is controversial (Ref. 27). In addition, antennas or optical systems are needed with sensing equipment and these systems are expensive, heavy and require more than ten watts of power.

7 - SYSTEM IMPACT ON LRV

7.1 EFFECT OF SYSTEM ON MISSION REQUIREMENTS

In discussing the effect of the hazard detection system on mission requirements the system has to be considered in two different parts, the surface system and the sub-surface system.

For surface hazard detection a candidate system is FM-CW Radar. The FM-CW Radar system as proposed appears feasible and is within the near state-of-the-art. The system will provide a range capability of approximately 3 meters and resolution to approximately 1/2 meter. Thus, it will be capable of detecting surface formations considered hazardous to a vehicle travelling in the unmanned mode. A faster moving vehicle would require detection of obstacles further in advance because of the need for increased breaking distance. In addition finer resolution would be required since at increased speed, smaller obstacles would effect the stability of the vehicle. Since 3 meters approximates the minimum turning radius of the vehicle it would be difficult to safely provide an automatic turning capability with this hazard detection system, particularly if the obstacle were in the center of the vehicle's path. This function would best be left up to the remote operator who after receiving an automatic stop signal would maneuver the vehicle and turn it into an obstacle free path. This hazard detection system would provide the operator with an indication of the direction of the obstacle.

The constraint of having to stop the vehicle at the detection of every obstacle will not appreciably degrade the mission requirement of a 1000km traverse capability. Using figures from Grumman's LRV project, the vehicle will have enough driving time to traverse 1155km at an average speed of 1.2km/hr after all times for lunar nights, adverse lighting conditions, scheduled stops and battery recharge are deleted from the total mission time. This excess of 155km at 1.2km/hr. converts into 160 hours. If a reasonable decision and maneuver time of 1/2 minute is assumed each time an obstacle is encountered, a total of 19,200 obstacles or one every 50 meters could be encountered before the 1000km mission requirement would be degraded.

Statistical data on lunar formations in the mission areas of concern (Ref. 28) show that the distribution frequency of positive obstacles is approximately 1 per 100 meters and negative obstacles approximately 3 per 100 meters. From this data it can be concluded that the mission traverse requirement of 1000km would be degraded by as little as 150km if the vehicle stopped at every obstacle encountered. However, a realistic assumption is that

many of the large obstacles encountered would be readily discernable with remote T.V. far enough in advance so that avoidance maneuvers could be executed negating the need to stop at these obstacles.

Sub-surface hazards can theoretically be detected by either the seismic or soil penetrating radar schemes. The speed of the vehicle would be limited by the amount a boom could be extended for the radar scheme and by the geophone wheel noise of the seismic scheme. Considering these restraints, the schemes would be limited to the unmanned mode of operation. Both schemes as presented would add to the turning radius of the vehicle and would decrease the maneuverability of the vehicle. In addition, surface hazard detectors would have to be moved forward to protect these mechanisms.

Both schemes are prone to false alarms because of the difficulty in discerning between forward range and depth in the seismic scheme and hazard size in the radar scheme. Thus, either scheme if utilized would require the vehicle to stop at the detection of any void and the operator to maneuver the vehicle into a new direction and try again. In summary, the sub-surface hazard schemes would be restricted to the unmanned mode, would increase its turning radius and would cause numerous stops if sub-surface voids proved statistically high. The effect of these systems on the mission traverse requirement of the LRV can not be postulated at this time since data on the distribution frequency of sub-surface voids is non-existent.

7.2 COMPATIBILITY OF SYSTEM WITH LRV SPACE, WEIGHT AND POWER REQUIREMENTS

The FM-CW radar scheme was selected because it will meet the space ($<1 \text{ ft}^3$), weight ($<10 \text{ lbs}$) and power ($<10 \text{ watts}$) guide lines set down by the LRV project and would be mounted as shown in Figure 1. If the restriction on power were relaxed then the range and resolution could be improved. The range improvement would be realized since the increased power would overcome the increased free space loss and decreased surface reflection. The resolution improvement would be possible since the increased power could provide higher antenna gains which along with narrow beams could provide finer resolution. It should be pointed out however, that if the space, weight and power requirements were relaxed and the future state-of-the-art provided an all solid-state pulse system, the pulse system would provide better performance than the FM-CW system. This performance advantage would be realized in resolution since the pulse system does not possess the inherent step error of the FM-CW system.

In the case of sub-surface hazard detection schemes the power guideline can be met with soil penetrating radar if the lunar soil losses do not exceed theoretical values and

can be met with the seismic scheme if signal processing requirements do not prove excessive. The size and weight requirements would be exceeded by both schemes. The radar scheme requires large antennas and a boom extension whereas the seismic scheme requires extra wheels and coupling to the vehicle (Fig. 14).

Further studies may provide some improvement in these areas. A determination of the highest frequencies which would allow meaningful penetration into the lunar soil would provide some reduction in the radar antenna size. The acquisition of reliable reflection data at angles other than normal incidence could permit the antenna to be mounted closer to the vehicle. In the case of seismic, testing of geophone arrangements and isolation methods may provide a scheme where the geophones could be mounted within the envelope of the vehicle.

7.3 ANCILLARY EQUIPMENT REQUIREMENTS

The discussion on ancillary equipment will be limited to the FM-CW system. The block diagram of Figure 18 shows the minimum logic needed for a reliable surface hazard detection system. It assumes an array of six sensors each of which will be sequentially gated on and off by inputs from the synchronizer. This rate of synchronization can be adjusted to vehicle velocity by inputs from an odometer or digital tachometer. Each sensor will have its own logic channel. It will not be enough to have a threshold detector which will trigger at discrete positive or negative thresholds. Analysis in the study has shown that the greatest probability of false alarms will come from negotiable slopes. It does not matter how fine a resolution the system has, there will be a point in the vehicle's approach to a negotiable slope when the return from that slope will exceed the obstacle threshold. In order to overcome this false alarm problem successive readings must be compared to show that the change does or does not exceed a threshold rate. A simple circuit regulated by the synchronizer would cause the first return to be clamped in a hold circuit until the receipt of the subsequent returns. The subsequent returns would pass the hold circuit and subtract from the first return at the output of the hold circuit. These differences over the rate determined by the synchronizer and the vehicle speed would indicate the change of slope. Thus, if the system detected an object whose rate of change in return indicated a non-negotiable slope and whose magnitude of return exceeded that of a non-negotiable obstacle an AND gate would be triggered sending a brake signal to the vehicle controls.

The FM-CW system does not offer any automatic turning capability to the control system but each channel can be monitored so that the controller will have an indication of the direction of the hazard.

The pitching and rolling of the vehicle will raise the possibility of false alarms. The error analysis of the FM-CW system indicated that variations in pitch and roll from

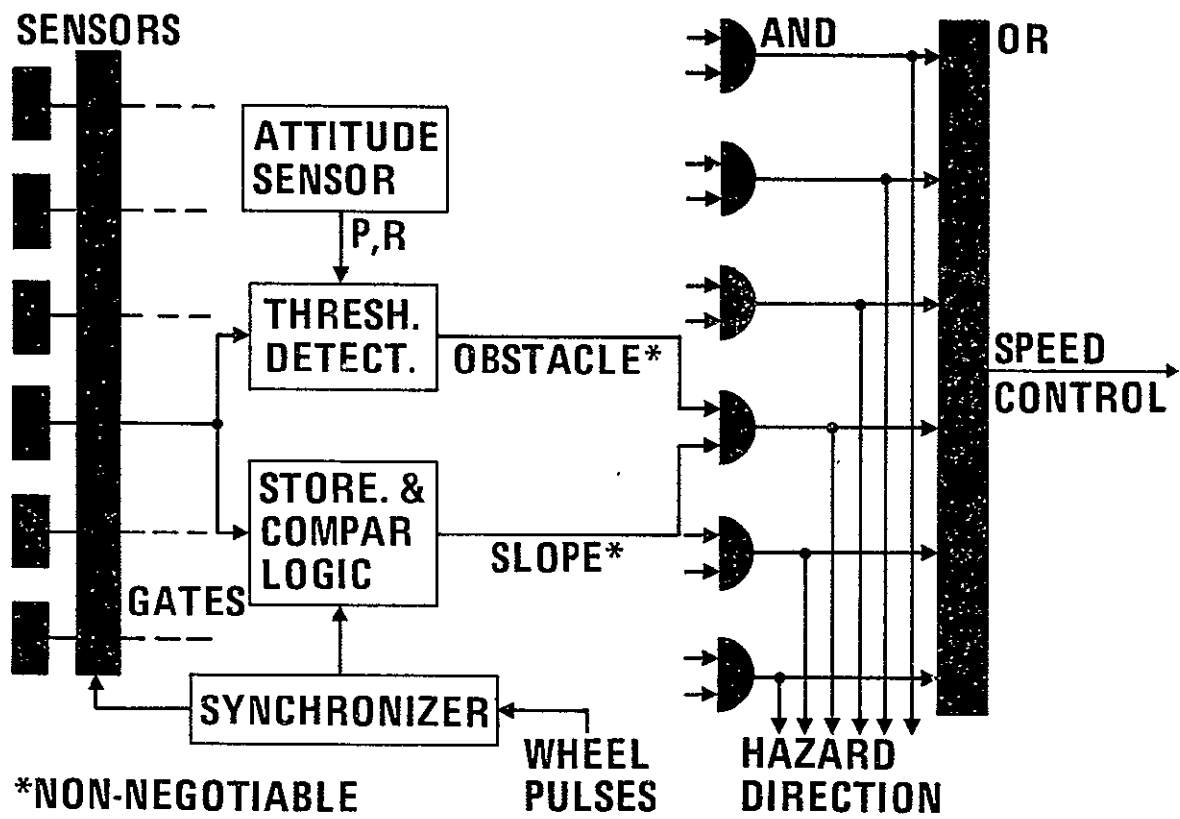


Figure 18. Minimal Hazard Detection System

1 to 2 degrees would effect the false alarm rate. If the final vehicle configuration shows that pitch and roll variations greater than this can be expected then compensation to the threshold bias must be added. This compensation could be supplied by vertical sensors which have accuracies up to 2° or by sun sensors which have accuracies up to 0.5° . In addition to reduction in the false alarm rate the attitude sensors would also provide compensation to the rate of change of slope threshold. This would be necessary since if the vehicle was already proceeding along a negotiable slope, the threshold for a change in slope would then be less than 35° . Attitude sensors such as these are presently being considered for incorporation into the navigation and control systems of the LRV. Thus, the ancillary equipment required for the hazard detection system is well within the state-of-the-art and requires a minimum of sophistication.

8 - RECOMMENDATIONS

It is recommended that the RF effort for surface hazard detection be carried into a lab and system evaluation stage. In the laboratory phase a determination will be made of optimum operating frequencies. These operating frequencies include the transmitting or carrier frequency, the modulating frequency and the rate of deviation or sweep. Standard microwave test equipment will be used to provide various combinations of frequencies. Selection of frequencies will be based on those providing the best resolution and minimum step error at the ranges of interest with minimum complexity and state-of-the-art equipment used as trade-off parameters. Antenna configurations will also be tested in this phase. Various sizes and shapes will be evaluated with different frequency combinations. Minimum size offering the finest resolution will be the goal of this evaluation. Antenna arrays will be evaluated to determine their capability to provide the required resolution and azimuthal coverage. Isolation techniques to insure minimum leakage between transmit and receive antennas will also be evaluated in this phase. All tests conducted during this phase will be performed at controlled target sizes and ranges to insure proper evaluation of the various parameters.

A development model would then be fabricated utilizing available equipment that would most closely approximate the characteristics determined in the lab evaluation and which would be compatible with the LRV configuration. The development model would be mounted aboard Grumman's prototype LRV. System tests would then be conducted at Grumman's simulated lunar landscape. The hazard detection system would be evaluated under dynamic conditions. Optimum mounting configurations would be selected and a determination made of the compensation needed for pitch and roll.

Concurrent with the system evaluation it is recommended that a detailed design of the interface logic be formulated. This design would include the gating circuitry, synchronizer, threshold detectors, biasing circuitry, and control and display logic to interface the hazard detection sensors with the LRV mobility controls. A development model would be fabricated from this design and mounted on the vehicle during system evaluations. Standard attitude sensors would be evaluated and modified for incorporation into the hazard detection system. Gains and scaling factors would be selected to provide adequate compensation for pitch and roll.

It is recommended that the investigation into sub-surface hazard detection be continued. In the seismic area various seismic signal sources would be fabricated and field

tested in conjunction with selected geophone configurations. The tests would be conducted over known geophysical formations so that the response to various types of sub-stratifications can be determined. The results of these tests would be utilized to formulate the type of signal processing that would be necessary to incorporate the responses into an automatic detection scheme. Concurrent with this phase, seismic results from Apollo 12 and later experiments would be monitored. This investigation would provide information as to what kind of seismic signals are to be expected and possibly what kinds of voids exist on the moon. The Grumman Aerospace Corporation has had extensive experience utilizing various types of signal processing to detect weak sine wave type signals in noise. A data reduction center is currently in operation in Bethpage studying such signals on a classified military program.

The seismic program would also include an investigation of noise isolation methods for the geophone sensors. Isolation would be necessary if the geophone sensors were to be mounted on the actual driving wheels of the vehicle.

The goal of the recommended seismic study would be to provide a design of a completely automatic seismic detection system capable of being mounted within the envelope of the vehicle.

Further sub-surface hazard detection studies are recommended in the area of soil penetrating radar. Investigations would be carried out to determine the maximum transmitting frequency that could be utilized to provide meaningful penetration into the lunar soil. This would be correlated with lunar soil cohesion data and data on the overburden which the LRV presents to the lunar soil. The results of this phase of the study would be used to establish the threshold depth of a sub-surface void that would constitute a hazard and the smallest antenna size that could be used to penetrate this depth.

It is recommended that data on reflections from angles other than normal incidence be acquired. This data would be utilized to determine the increased soil reflection loss and the processing required to filter the desired signal from the expected complexities in the return waveform.

The study would include an investigation of state-of-the-art soil penetrating radars to determine how present processing and display techniques could be modified and adapted to an automatic hazard detection system.

The goal of the recommended soil penetrating radar study would be to provide a design of a completely automatic soil penetrating radar system capable of being mounted within the envelope of the system.

9 - REFERENCES

- (1) Saunders, W. K., Post-war Developments in Continuous-wave and Frequency-modulated Radar, IRE Transactions, Vol. ANE-8, March 1961.
- (2) On the Apollo 11 LM5 Data Analysis, Report No. 53966-126, Appendix IV, prepared by Ryan Aeronautical Company, San Diego, California, for RCA and Grumman Aerospace Corporation, on LM Contract NAS 9-1100, October 1969.
- (3) Skolnik, M. I., Introduction to Radar Systems, McGraw Hill, Inc., N.Y., 1962.
- (4) Wimberly, F. T., Lane, J. F., The AN/APN-22 Radio Altimeter, IRE Transactions, Vol. ANE-1, No. 2, June 1954.
- (5) ITT Handbook, Reference Data for Engineers, Fifth Edition, Howard Sams and Co., Inc., N.Y., 1968.
- (6) Proposal for Radar Altimeter, General Dynamics Electronics, San Diego, California, 1969.
- (7) Parasnis, D. S., Principles of Applied Geophysics, John Wiley, 1962.
- (8) Cook, J. C., Seismic Mapping of Underground Cavities Using Reflection Amplitudes, Geophysics, Vol. 30, No. 4, pp 527-538.
- (9) Tubbs, D. W., Personal communication, 1969.
- (10) Zack, A., The Detection of Sub Surface Openings Using Gravinometric and Seismic Techniques, Thesis, Vanderbilt U., June 1967.
- (11) Porter, C. O., Electrical Resistivity Investigations over Limestone Caverns, Thesis, Texas A & M, May 1966.
- (12) Egemier, S. Personal communication, 1969.
- (13) Watkins, J. S., Godson, R. H., and Watson, K., Seismic Detection of Near Surface Cavities, U. S., Geological Survey Professional Paper 599-A, 1967.
- (14) Watkins, J. S., Godson, R. H., and Watson, K., Seismic Investigation of Near-Surface Cavities - A Preliminary Report, Bulletin Nat. Speleological Society, V 28, P 94, 1966.
- (15) Biot, M. A., Propagation of Elastic Waves in a Cylindrical Bore Containing a Fluid, Jour. Appl. Physics, V 23, pp 997-1005, 1952.
- (16) Rinker, J. N., Radio Ice-Sounding Techniques, U. S. Army Cold Regions Research and Engineering Laboratory, Proceedings of the Fourth Symposium on Remote Sensing of Environment, Michigan University, April 1966.

- (17) Nikodem, H. J., Effects of Soil Layering on the Use of VHF Radio Waves for Remote Terrain Analysis, U. S. Army Engineer Waterways Experiment Station, Proceedings of the Fourth Symposium on Remote Sensing of Environment, Michigan University, April 1966.
- (18) Feder, A. M., Programs in Remote Sensing of Terrain, Texas Instrument Inc., Proceedings of the Second Symposium on Remote Sensing of Environment, Michigan University, Oct. 1962.
- (19) Holdsworth, D. W., and Barringer, A. R., Studies of the Radar Properties of Rocks in Vacuum and the Design of Specialized Radar for Measuring Stratification Features of the Lunar and Terrestrial Surface, Barringer Research Inc., Proceedings of the Fourth Symposium on Remote Sensing of Environment, April 1966.
- (20) Meyer, Dr. M., Remote Sensing of Ice and Snow Thickness, Adcole Corporation, Proceedings on the Fourth Symposium on Remote Sensing of Environment, April 1966.
- (21) Cook, J. C., Monocycle Radar Pulses as Environmental Probes, Southwest Research Institute, Proceedings of the Second Symposium on Remote Sensing of Environment, Oct. 1962.
- (22) Electromagnetic Tunnel Detector, Model 197-2, Technical Report to U.S. Army Mobility Equipment Research and Development Center, Fort Belvoir, Va., Contract No. DAAK 02-68-C0143, General Dynamics Electronics, San Diego, Calif., 1969. (Conf.)
- (23) Von Hippel, A., Dielectric Materials and Applications, John Wiley and Sons, Inc., 1958.
- (24) Olson, W. E., Personal communication, 1969.
- (25) Thraikill, J., Personal communication, 1969.
- (26) Kennedy, J. M., A Microwave Radiometric Study of Buried Karst Topography, GSA BULLETIN, V 70, No. 6 (Geological Soc. of Amer.)
- (27) Tubbs, D., REVIEW, NSS NEWS, Vol. 27, No. 7, p 101, July 1969, (National Speleological Society).
- (28) Moore, H. J., Pike, R. J., Ulrich, G. E., Lunar Terrain and Transverse Data for Lunar Roving Vehicle Design Study, prepared by the Geological survey for the National Aeronautics and Space Administration, March, 1969.

10 - BIBLIOGRAPHY

1. Chanzit, L., et al, Study of Airborne Millimeter Radar Techniques, Quarterly Report, United Aircraft Corp., Norwalk, Conn., January 1968.
2. Hata, M., Some Design Criteria to Obtain High Resolution of FM Radar, Electronics and Communications in Japan, Vol. 50, October 1967.
3. Edwards, J. A., Withers, M. J., High Resolution FM-CW Radar for Emergency Vehicle Guidance in Fog, Institution of Electrical Engineers/ IEE Conference Publication No. 28, London, England, March 1967.
4. Evans, J. V., Hagfors, T., Study of Radio Echoes from the Moon at 23 Centimeters Wavelength, Journal of Geophysical Research, Vol. 71, October 1966.
5. Wachter, J. F., Collision Avoidance in Restricted Visibility, Institute of Navigation Journal, Vol. 19, July 1966.
6. Foreman, D. E., Sedivec, D. F., Experimental Observation of the Creeping-Wave Phenomenon in Backscatter Using a Short-Pulse Radar System, IEEE, Proceedings, Vol. 53, August 1965.
7. Davis, J. R., et al, Decameter-Wave Radar Studies of the Lunar Surface, Journal of Research, Section D, Radio Science, Vol. 69D, December 1965.
8. Cann, A. J., CW-Equivalent Radar Cross-Section Measurements with a Pulse, IEEE, Proceedings, Vol. 53, October 1965.
9. Cook, E. J., Hardin, C. D., A Miniature Millimeter Wave Magnetron and Its Applications, Proceedings of the National Aerospace Electronics Conference, Dayton, Ohio, May 1964.
10. Craig, S. E., High Range Resolution Coherent Radar, Radar Division, U. S. Army Signal Research and Development Laboratory, Fort Monmouth, N. J., June 1964.
11. Milburn, J., Short Pulse Model Measurement Studies, Final Technical Report, General Dynamics Corporation, Fort Worth, Texas, October 1966.
12. Chanzit, L., et al, Study of Airborne Millimeter Radar Techniques, Quarterly Report, United Aircraft Corp., Norwalk, Conn., July 1966.
13. Chanzit, L., et al, Study of Airborne Millimeter Radar Techniques, Quarterly Report, United Aircraft Corp., Norwalk, Conn., October 1966.
14. Cragon, H. G., Large Scale Integrated Circuit Array, Interim Technical Report No. 1, Texas Instruments, Inc., Dallas, Texas, April 1966.

15. Cutrona, L. J., Experimental High Resolution Radar and Related Items, Interim Engineering Report No. 3, Conductron Corp., Ann Arbor, Michigan, March 1963, (Conf.).
16. Alongi, A. V., Kell, R. E., Newton, D. J., A High Resolution X-Band FM-CW Radar, Cornell Aeronautical Lab, Inc., Buffalo, N. Y., Michigan University Radar Symposium Record, August 1964, (SECRET).
17. Caputi, W. J., Van Deusen, R. B., High Resolution Stretch Radar, Cutler-Hammer, Inc., Deer Park, N. Y., Michigan University Radar Symposium Record, August 1964, (SECRET).
18. Downey, J. A., Tiffany, O. L., Zaitzeff, E. M., Scientific Exploration of the Moon Using a Roving Vehicle, Proceedings of the 11th Annual Meeting of the American Astronautical Society, Chicago, Illinois, May 1965.
19. Koryagin, V. V., Phase Distortions of Reflections at Short Times in Grouped Detonations, Air Force Systems Command, Wright-Patterson AFB, Ohio, November 1967.
20. Project VT/4051, Interim Report, Teledyne Industries, Inc., Garland, Texas, June 1964.
21. Lowrie, L. M., Mickey, M. V., Strong-Motion and Surface Accelerations, Project Handcar, Coast and Geodetic Survey, Washington, D. C., November 1965.
22. Bryusov, B. A., Interpretational Possibilities of the Method of Statistical Correlation of Gravimetric and Seismic Data, Aeronautical Chart and Information Center, St. Louis, Mo., January 1967.
23. Clinard, R. H., Lunar Geophysical Surface and Subsurface Probes for Apollo Applications Program-Volume I, Texaco Experiment, Inc., Richmond, Va., May 1966.
24. Riecker, R. E., Bibliography of Experimental Rock Deformation, Second Edition, Part II, Terrestrial Sciences Lab, Air Force Cambridge Research Labs, Bedford, Mass., August 1966.
25. Keotser, D. J., Improved High-Resolution Seismic Profiling, Dept. of Geology and Geophysics, Massachusetts Institute of Technology, Cambridge, Mass., June 1966.
26. Manned Lunar Exploration Investigations, Semi-annual Report, Geological Survey, Washington, D.C., January 1965.
27. De Bremaecker, J. CL., Kane, M. F., Watkins, J. S., Examination of the Lunar Near-Surface Rocks By Engineering Seismic Techniques During Early Appollo Landings, Geological Survey, Flagstaff, Arizona, January 1965.
28. De Bremaecker, J. CL., et al, Investigation of in Situ Physical Properties of Surface and Subsurface Site Materials by Engineering Geophysical Techniques, Annual Report, Geological Survey, Flagstaff, Arizona, Fiscal Year 1965.

29. Godson, R.H., Loney, R.A., Watkins, J.S., Investigation of in Situ Physical Properties of Surface and Subsurface Site Materials By Engineering Geophysical Techniques, Annual Report, Geological Survey, Flagstaff, Arizona, Fiscal Year 1964.
30. Ackermann, H.D., Godson, R.H., Watkins, J.S., Seismic Survey of Meteor Crater, Geological Survey, Flagstaff, Arizona, February 1966.
31. Apollo Lunar Science Program, Report of Planning Teams, Part II - Appendix, National Aeronautics and Space Administration, Washington, D.C., December 1964.
32. Report of Geophysics Working Group, Summer Conference on Lunar Exploration and Science, National Aeronautics and Space Administration, Washington, D.C., 1965.
33. Williams, O.W., A Compendium of Papers in the Fields of Wave Propagation and Geotechniques Prepared at AFCRL During 1963, Terrestrial Sciences Lab, Air Force Cambridge Research Labs, Bedford, Mass., December 1964.
34. Crowe, C., Westhusing, J.K., Techniques for Lunar Water Exploration, Final Report, Texas Instruments, Inc., Dallas, Texas, September 1964.
35. Romberg, F.E., et al, Evaluation of Lunar Gravity Needs and Gravity Meter Capabilities, Texas Instruments, Inc., Dallas, Texas, August 1963.

APPENDIX A

Surface Hazard Detection Analyses

- A.1 Threshold Logic for Slopes
- A.2 Errors in Surface Hazard Detection
- A.3 Detection Probability and False Alarm Rate

APPENDIX A

A.1 THRESHOLD LOGIC FOR SLOPES

The following section discusses the problems that exist in the detection of slopes and the modifications that must be made to the threshold logic to minimize these problems. The section is divided into two parts, negative slopes and positive slopes, since each detection situation will require its own threshold logic considerations.

A1.1 Negative Slopes

Figure 19A depicts the vehicle approaching a negative slope of 25° in a simple flat terrain and flat slope situation. The range reading will not increase until the beam (Point R) reaches the start of the slope, Point O. As the forward half of the beam (Segment CR) proceeds down the slope, the range reading will increase only slightly. This is due to the fact that the reflection coefficient decreases approximately 1 db per 5° decrease of incidence angle (Figure 4). Thus, when the centerline of the beam, Point C, has reached Point O, the relative weight of the return from the forward half of the beam compared with that of the total beam is 5 db down from .50 or .16. Since the forward half of the beam, alone, has undergone a .15 meter increase in range, the total range increase is $.15 \times .16$ meters, or about .024 meters. When the vehicle travels another .25 meters Point L of the beam has reached Point O, and the complete beam is now illuminating the slope (Figure 19B). The increase in range per travel distance of .25 meters is given by:

$$QC = \frac{QM}{\sin(\phi - \alpha)} = \frac{.25 \sin \alpha}{\sin(20^\circ)} = \frac{.25 \sin 25^\circ}{\sin 20^\circ} = .308 \text{ meters}$$

where: ϕ = depression angle

α = slope angle

This is equivalent to or 7.25% of reference range. In each subsequent 0.25 of travel (on the level terrain) the range reading will increase by .308 meters. (But the amplitude of the return will be 5 db down from the reference return due to decreased reflection coefficient.) When the vehicle has traveled .25 meters and the wheelbase is at Point O the total range increase will be $9 \times .308$ or 2.77 meters. This will result in an additional 4.34 db decrease in return power, making the return power 9.34 db down from the reference return, before the vehicle itself enters the slope and the amplitude of the return is increased again. This points up the fact that the receiver should respond to signals at least 9.34 db lower than the reference signal. Since the amplitude of the signal return from 35° slopes (which are negotiable by the vehicle) will be lower than that for the 25° slopes they will, in all proba-

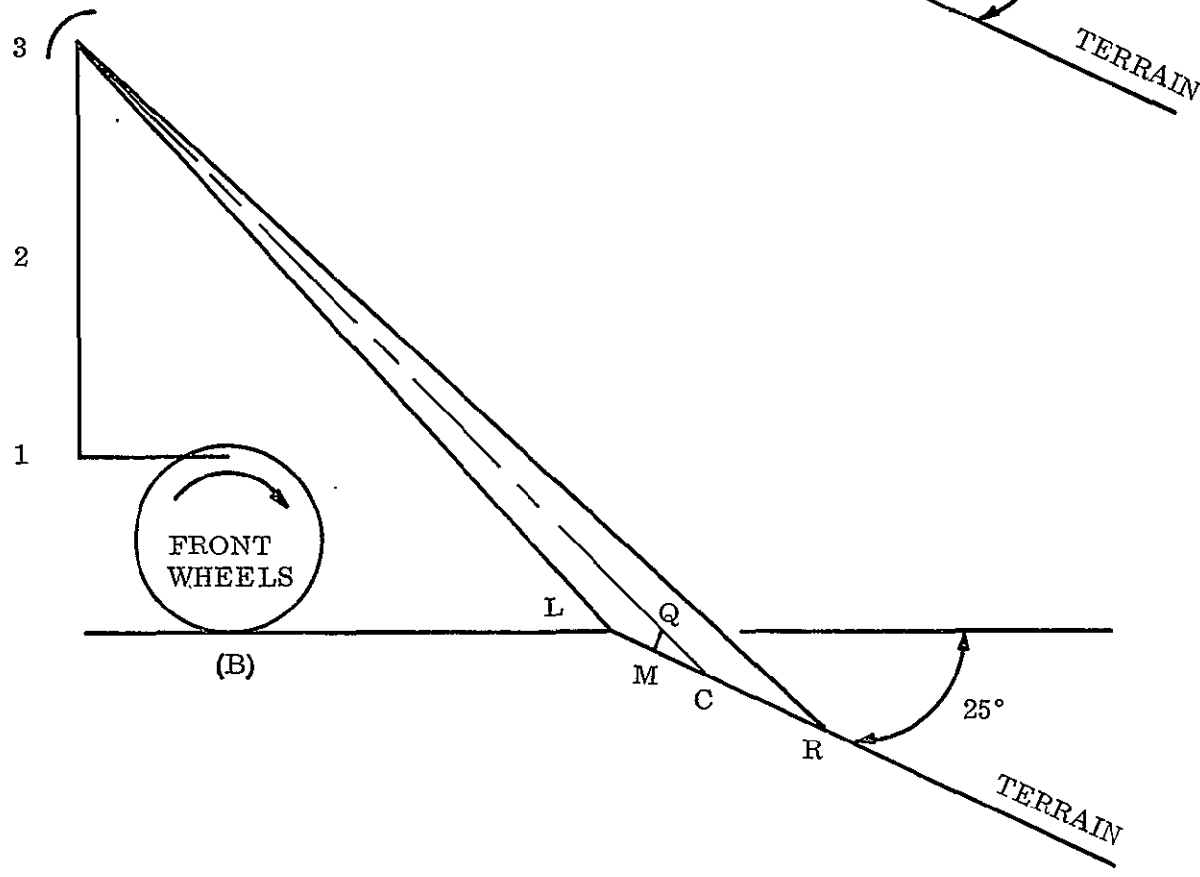
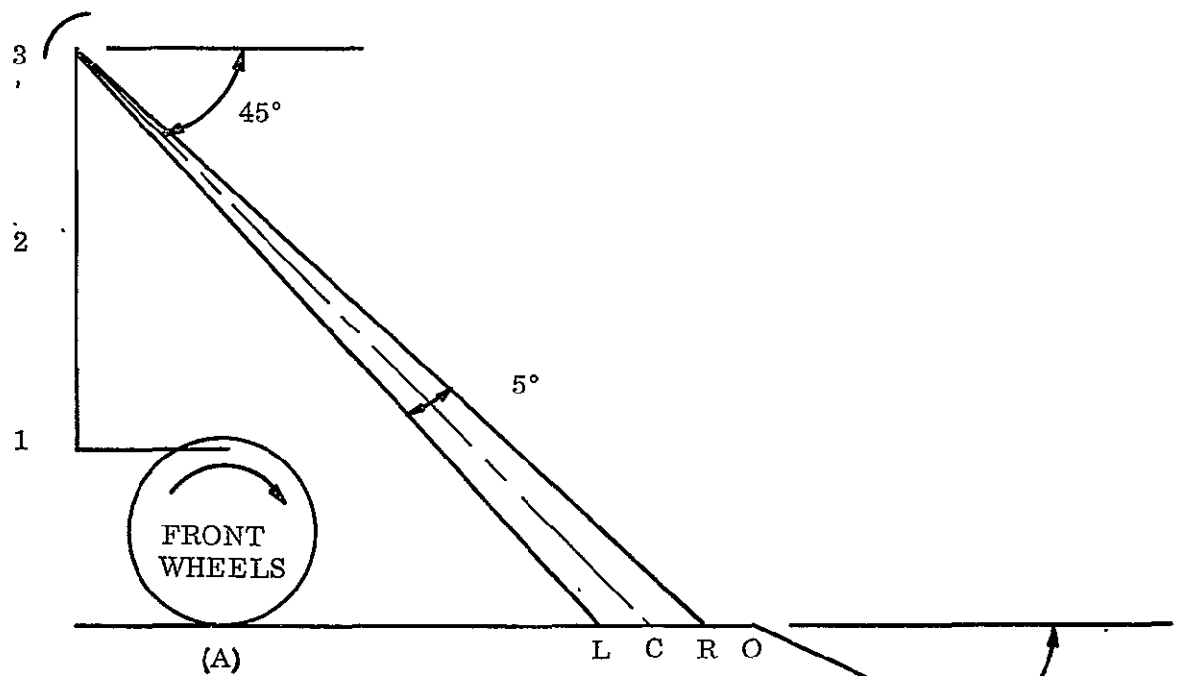


Figure 19. Vehicle Approaching 25° Slope

bility, be below threshold as the vehicle wheelbase approaches the start of the slope. Thus, they will not be detectable by the radar, and will therefore be identified as hazards. 25° slopes will however be detected by the radar if the receiver will respond to signals that are 10 db below the returns from level terrain. The slope problem requires that in addition to obstacle threshold detection the radar system must include slope measuring logic.

In the case of negative slopes the logic will be adjusted so that range increases of more than 0.85 meters per 0.5 meters of travel or less would indicate a hazardous slope. (This value is discussed in Sec. A.3). A range reading will be taken every 0.25 meters of vehicle travel (diode switching rate of 2 cycles per second) and range differences will be measured between the first and two subsequent readings, covering a total travel distance of 0.5 meters. The one meter hole represents a special case of a negative slope in which the slope angle is 90°, but the reflecting surface is the opposite vertical wall (Refer to Figure 20). Consider the case when the beam has just reached the edge of the hole, (Fig. 20A) i.e. Point R is over the left side of the hole. As the vehicle moves forward another 0.25 meters, the forward half of the beam will be completely inside the hole (Point C, the beam centerline, will be over the left side of the hole) and will be reflected back from the right side of the hole, while the trailing half of the beam is reflected from the level terrain. Under these conditions the return energy from the forward part of the beam may or may not be larger than that from the trailing half of the beam, depending on the reflection coefficient from the right side of the wall.

Assume, for example, that the return from the forward half of the beam is 3 db less than that from trailing half of the beam. The weighted return from the forward half of the beam compared to the return from the total beam is then .50x.50 or 1/4 the total weight. Since the front half of the beam undergoes about a 1.30 meter increase in range reading, the weighted increase in range is about 1/4x1.30 meters or .33 meters, and the hole is not yet sensed as a hazard. However, during the next 0.25 meters of vehicle travel, the trailing half of the beam, enters the hole, so that the complete beam has just entered the hole. (Figure 20B). Under these conditions the range increase, above the reference or level range, is about 1.10 meters, and the condition is identified as a hazardous slope. It should be noted, that although vertical sided walls have been assumed for simplicity, other walls making different angles, will not materially affect the analysis presented here.

The foregoing analysis shows that for a vehicle traversing a flat terrain, discernment between negotiable negative slopes and non-negotiable negative obstacles or slopes can be made for slopes as steep as 25° with the proper implementation of threshold logic. Restrictions imposed by line-of-sight will prevent discernment of slopes between 25° and 35°.

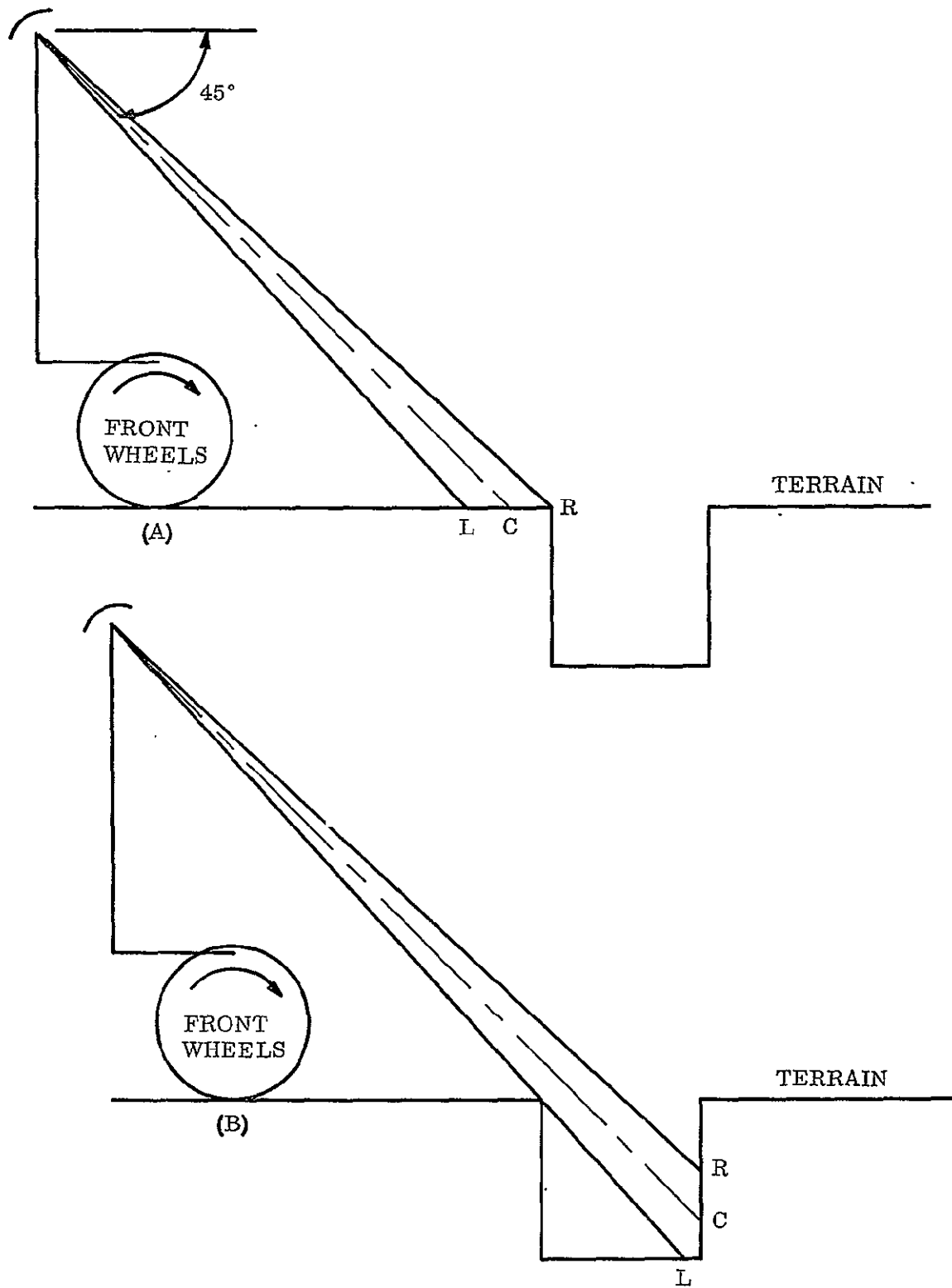


Figure 20. Vehicle Approaching One Meter Hole

A.1.2 Positive Slopes

The detection of positive slopes is less of a problem than the detection of negative slopes, due to the fact that the reflected power increases as the slopes are approached (about 1 db increase per 5° of slope). Figure 21A depicts the vehicle approaching a positive slope of 35°. As shown in the figure the beam (ray R) has just reached the start of the slope, Point O, and the range reading will now decrease as the vehicle travels further. Figure 21B shows the situation a short time later when the vehicle has moved 0.50 meters. The decrease in range reading is given by:

$$QC = QM \frac{\sin \alpha}{\sin (\phi + \alpha)} = \frac{.50 \times \sin 35^\circ}{\sin (80^\circ)} = .292 \text{ meters.}$$

(ϕ is the depression angle and α is the slope angle).

Since this decrease is a relatively small amount, the range decrease must be measured over a longer distance of vehicle travel. For example, the measured range decrease over a 1.75 meter travel approach to a 35° slope would be 1.02 meters. The radar logic (for positive slopes) will therefore be adjusted so that if the range decrease is more than .77 meters per 1.75 meters of travel or less, the slope is identified as hazardous. (This value is discussed in Sec. A.3). A range reading will be taken every 0.25 meters of vehicle travel and range differences will be measured between the first and seven consequent readings, covering a total travel distance of 1.75 meters.

Allowing therefore, 1.75 meters of travel to determine whether the slope is negotiable, the vehicle will then have to be halted (after application of braking signal) in a distance of 0.25 meters or less. This is within the capability of the vehicle on level terrain. The 1 meter obstacle hazard represents a special case of a positive slope wherein the slope is 90° (refer to Figure 22A). Consider the case when the beam has just reached the obstacle (i.e. point R in contact with the base of the obstacle). As the vehicle moves forward 1.0 meters (Figure 22B) the maximum range decrease will be about 1.1 meters and the system will indicate a hazard.

The foregoing analysis shows that for a vehicle traversing a flat terrain, discernment between all negotiable positive slopes and non-negotiable positive obstacles or slopes can be made with proper implementation of threshold logic.

A.2 ERRORS IN SURFACE HAZARD DETECTION

Errors in range readings will be due to pitch error, roll error, terrain random roughness (power spectral density), terrain random slope angle and inherent radar errors. The following section discusses each of these sources of error in detail and then summarizes

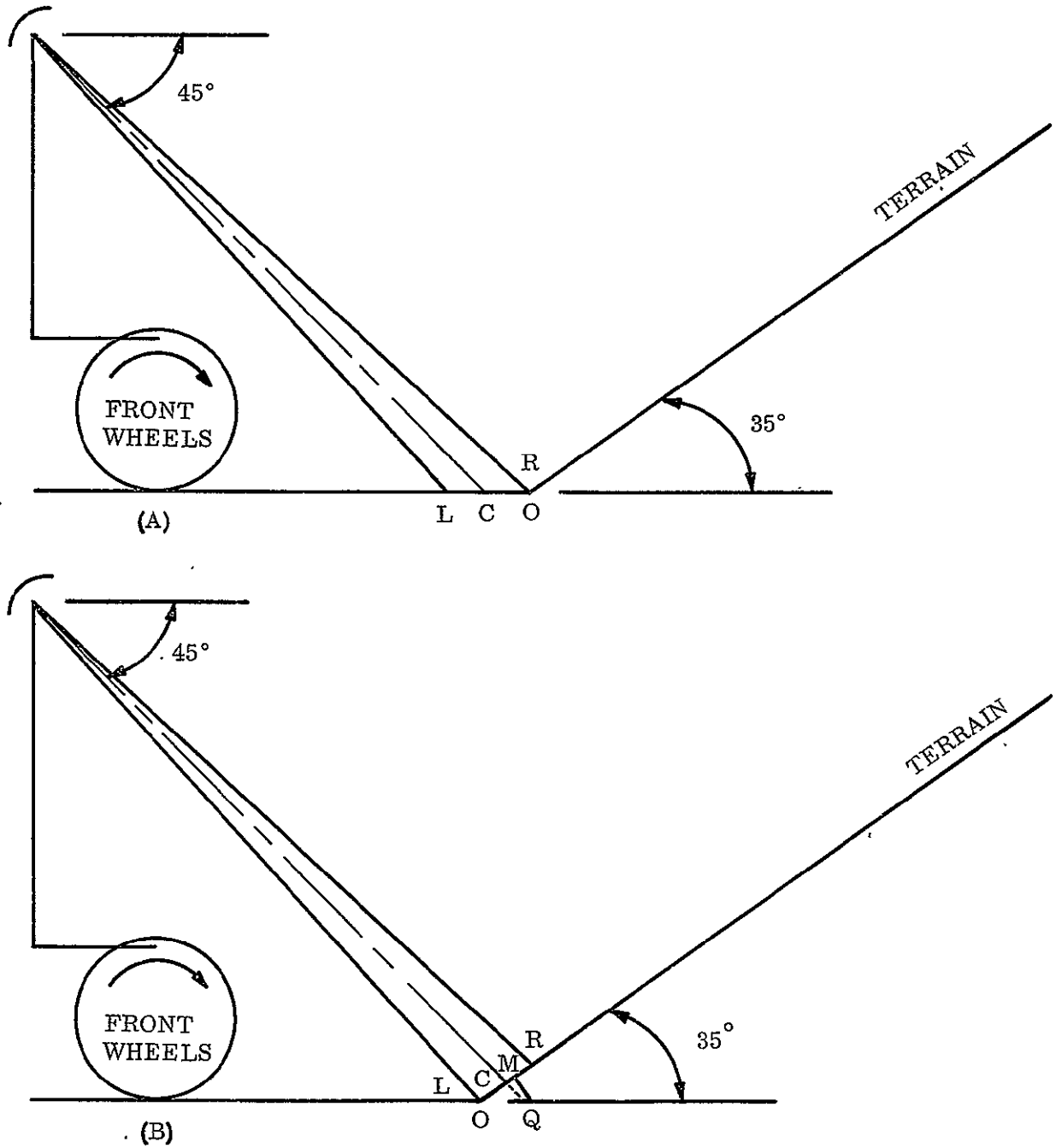


Figure 21. Vehicle Approaching 35° Slope

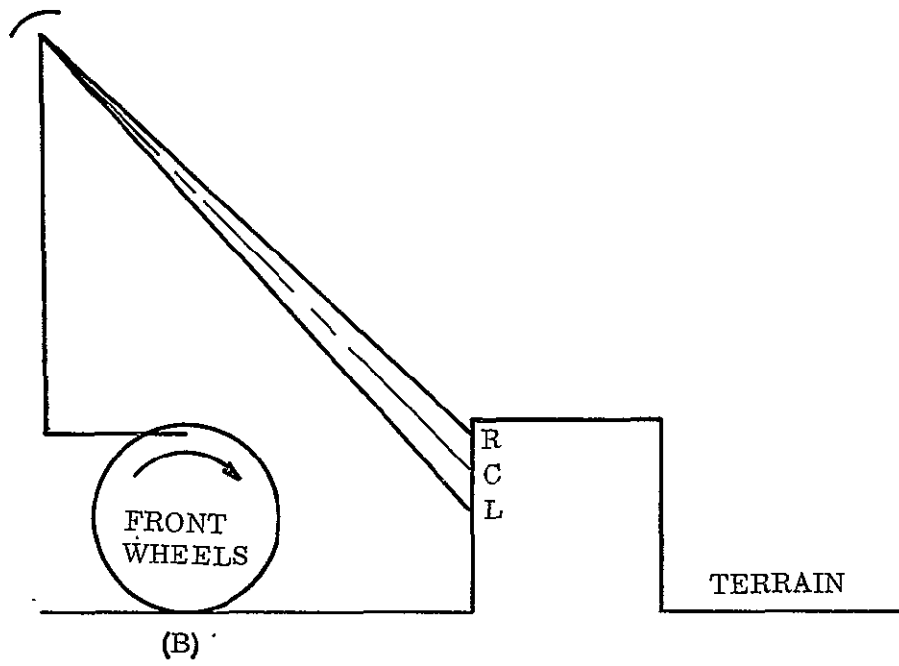
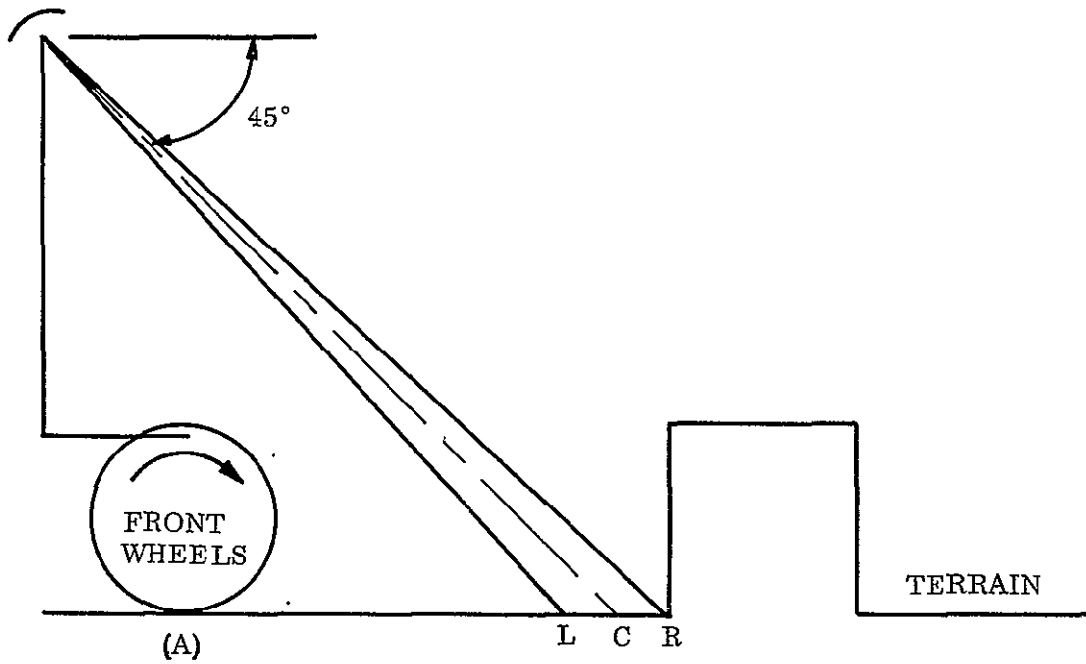


Figure 22. Vehicle Approaching One Meter Block

the combined effect they would present to a surface hazard detection system. Inherent radar errors are discussed in section 5 and the results from that analysis are also included in the final summation of errors.

A.2.1 Vehicle Pitch and Roll

Erroneous range indications will be produced when the beam depression angle, with respect to the horizontal (45°) varies, due either to vehicle pitch, pitching of the mast structure, or both. For example, if the depression angle increases by 1.5° from 45° to 46.5° , the slant range will decrease by $\frac{3}{\sin 45^\circ} - \frac{3}{\sin 46.5^\circ}$ or $\pm .10$ meters.

It is shown in section A.3 that in order to insure a reasonably high detection probability the total system errors must be less than .125 meters. Since pitch error is only one of a number of errors expected, an error of .10 meters would be unacceptably high. In order to assure a reasonable budget for the pitch error, compensation (using appropriate range bias voltages) must be provided for this pitch variation so that the effective variation in depression angle is less than $.75^\circ$. This would keep the maximum slant range error due to pitch change less than $\pm .0507$ meters. The RMS error would then be given by $\frac{2 \times .0507}{2 \sqrt{3}} = .0288$ meters.

Similarly, range reading errors will be produced when the vehicle rolls and causes the six transmit antennas to roll with it. The largest errors will be produced in the extreme antennas, Nos. 1 and 6, (see Figure 3). For example, assuming antenna No. 6 is 0.8 meters from the vehicle center line then the slant range error (to a first order) due to a roll of 2.5° is $0.8 \times \frac{\sin 2.5^\circ}{\sin 45^\circ} = \pm .05$ meters. Thus, if the roll is compensated to within 2.5° about its reference, or horizontal plane value, then the expected or RMS error would then be given by $\frac{2 \times .05}{2 \sqrt{3}} = .028$ meters.

A.2.2 Errors Due to Lunar Terrain

Reference 28 includes a description of the different types of lunar terrain. Heterogeneity of the lunar surface virtually precludes a complete numerical description of all types of terrain that might be encountered by a lunar roving vehicle. The only meaningful alternative is a sampling of representative lunar terrain types or classes. Thus far, the availability of large scale terrain data has limited the number of lunar terrain classes to four: smooth mare, rough mare, hummocky upland, and rough upland. Table 1, which has been extracted from reference 28, shows the topographic features typically included in each category. The following is concerned with parameters such as the mean slope values and the power spectral density of the terrain and their effect on range reading.

TABLE 1 FOUR-PART CLASSIFICATION OF LUNAR TERRAIN

MARE			
Smoother Mare	Rougher Mare	Hummocky Upland	Rough Upland
(1) many Eastern sites	(1) many Western sites	(1) older vasin rim material (Fra Mauro fm)	(1) younger basin rim
(2) dark mare material	(2) rille, dome & ridge areas	(2) older large craters	(2) younger large craters
(3) older, subdued craters	(3) fresh craters	(3) blanketed craters	(3) scarps
(4) low crater densities	(4) high crater densities	(4) older, subdued crater hash	(4) fresh crater hash
(5) craters with few blocks	(5) blocky craters	(5) outer rim slopes of large craters	(5) inner rim slopes of large craters
	(6) secondary swarms especially on rays	(6) crater floors & basin fill	(6) trenches & rifts
	(7) large crater rims		

A.2.2.1 The Power Spectral Density. (PSD)

The Power Spectral Density (PSD) expresses the relief frequency content of a terrain profile as a time series. Like slope curvature it is a measure of relative terrain roughness, and can be somewhat independent of absolute slope angle and regional slopes. Reference 28 expresses this measure as a full logarithmic graph of power spectral density, in meters²/cycle/meter, against frequency, in cycles/meter. Two curves, representing roughest and smoothest terrain conditions within each of the four main lunar terrain types, are presented. The following is an attempt, using simple assumptions, to ascertain range reading error produced by this type of terrain roughness. For the smooth mare, two curves bracket most terrain types encountered in this type of mare.

At a frequency of one cycle per meter, (this is a convenient frequency for the hazard detection study since it is concerned with measuring change of range in an interval of one meter of vehicle travel) .0004 is taken as the average PSD between the curves.

For simplicity, the terrain height variation is represented by a sine wave whose rms value is $\sqrt{.0004}$ or .02 meters. Assuming then that the vehicle's vertical excursions

(and, therefore, the antenna) will have an rms value of .02 meters, and similarly, that the terrain illuminated will have an rms vertical excursion of .02 meters, then the vertical component of the slant range will have an rms value of $\sqrt{.02^2 + .02^2}$ or .028 meters. (This of course assumes statistical independence between the terrain illuminated and the terrain under the wheels). From this an RMS value (noise amplitude) or error in slant range reading is calculated to be:

$$\frac{.028}{\sin(\text{depression angle})} = \frac{.028}{\sin(45^\circ)}$$

or .04 meters per meter of vehicle travel due to terrain power spectral density on the smooth mare.

For the rough mare the same procedure is followed. At a frequency of one cycle per meter a PSD of .0009 is taken as an average value between the two curves, then, continuing as before, the error in slant range will be .06 meters per meter of vehicle travel.

For the hummocky upland .0005 is taken to be the value of the PSD. The slant range error is then .044 meters per meter of travel.

For the rough upland, .0009 is taken for the PSD. The slant range error is then .06 meters per meter of vehicle travel.

A. 2. 2. 2 The Slope Angle

Measuring the departure of topography from the horizontal, slope angle is an absolute index of terrain roughness. Slope angles measured along a profile may be expressed either as absolute values or algebraic values, where slopes facing, for example, east are designated positive, and west-facing slopes negative. Since comparatively little is to be gained from using algebraic slopes, the slope angle data given here is expressed in absolute values. Reference 28 gives the predicted distributions of one meter slopes for four lunar terrain types whose mean slope values are known or estimated. Referring to the smooth mare, the mean slope for one meter base length is 2.9° . This represents a height change of .051 meters in a one meter base length. The RMS height change will be $\frac{.051}{\sqrt{3}} = .03$ meters above or below the level ground, and the slant range error will be $\frac{.03}{\sin 45^\circ} = .0425$ meters. For the rough mare the mean slope value is 5.3° per meter of base length, and the slant range error will be .077 meters. For the hummocky upland the mean slope value is 8.2° per meter of base length, and the slant range error will be .12 meters, and for the rough upland the mean slope value is 11.0° and the slant range error will be .16 meters.

A.2.3 Summary of Errors

The errors in range readings will be due to pitch error, roll error, terrain random roughness (power spectral density) terrain random slope angle, and inherent radar errors. For the purpose of simplicity, the composite RMS error of any one range measurement will be taken as the root mean square of the component errors. The overall RMS error (1σ error) of a range difference measurement will be the composite RMS error multiplied by the $\sqrt{2}$ since the difference measurement consists of two independent slant range readings. The following is a listing of the errors

Pitch Error		.029 meters	
Roll Error		.028 meters	
Radar Inherent Error	(sect. 5)	.053 meters	
		PSD (meters)	Slope Angle (meters)
Smooth Mare Terrain Errors		.04	.0425
Rough Mare Terrain Errors		.06	.077
Hummocky Upland Terrain Errors		.044	.12
Rough Upland Terrain Errors		.06	.16

$$\begin{aligned} & \text{Smooth Mare Total Errors} \\ \text{Composite RMS Error} &= \sqrt{.029^2 + .028^2 + .053^2 + .04^2 + .0425^2} = .088 \text{ meters} \\ \text{Overall RMS Error} &= .088\sqrt{2} = .125 \text{ meters} \end{aligned}$$

$$\begin{aligned} & \text{Rough Mare Total Errors} \\ \text{Composite RMS Error} &= \sqrt{.029^2 + .028^2 + .053^2 + .06^2 + .077^2} = .118 \text{ meters} \\ \text{Overall RMS Error} &= .118\sqrt{2} = .165 \text{ meters} \end{aligned}$$

$$\begin{aligned} & \text{Hummocky Upland Total Errors} \\ \text{Composite RMS Errors} &= \sqrt{.029^2 + .028^2 + .053^2 + .044^2 + .12^2} = .143 \text{ meters} \\ \text{Overall RMS Error} &= .143\sqrt{2} = .202 \text{ Meters} \end{aligned}$$

$$\begin{aligned} & \text{Rough Upland Total Errors} \\ \text{Composite RMS Errors} &= \sqrt{.029^2 + .028^2 + .053^2 + .06^2 + .16^2} = .183 \text{ meters} \\ \text{Overall RMS Errors} &= .183\sqrt{2} = .258 \text{ meters} \end{aligned}$$

A.3 DETECTION PROBABILITY AND FALSE ALARM RATE

It is clear that the problem of range measurement errors will lead to false alarms and a detection probability that is less than 100%. The most important criterion is the probability of detecting the hazard, and this, will have to be as high as possible.

In the following analysis a detection probability, for a particular terrain, is assumed and the distribution of errors are assumed to be gaussian. Next the probability of false alarms for the various hazards, are evaluated using the previously computed RMS errors. A false alarm is defined as the case when the radar reports a negotiable slope, hole, or obstacle to be hazardous. The gaussian distribution chart of reference 5 has been utilized in the analysis.

A.3.1 The Positive Slope and Obstacle

It was indicated in section A-1 that the logic circuitry, for the positive slope case, will measure the range differences between the first and seven subsequent readings, covering a travel distance of 1.75 meters. For a slope angle of 35° , the computed range difference is 1.02 meters over this interval. As a starting point, a detection probability of 98% is assumed, for positive slope angles of 35° on smooth mare terrain. Since the overall RMS error (1σ value) for the smooth mare is .125 meters, then for 98% detection probability the threshold is set at 2σ below 1.02, or .77 meters. Of course the false alarm rate will be relatively high. For example a positive slope of 20° (which produces a range difference reading of .66 meters, or $.88\sigma$ below the threshold setting) will have a detection probability, or in this case, false alarm rate of about 20%. Slopes larger than this, will of course have higher false alarm rates.

Obstacles are basically in the same category as slopes and will be governed by the same logic. One meter height obstacles will register a range difference of 1.1 meters in the first 1.0 meter of travel and therefore have a probability of detection of about 99.5%. On the other hand 1/2 meter height obstacles, (which do not constitute hazards) will give a maximum range difference of about 0.68 meters (or $.72\sigma$ below the threshold reading) and will therefore have a false alarm rate of 24%. Larger blocks will of course have higher false alarm rates.

A. 3. 2 The Negative Slope and Obstacle

It was indicated in section A-1 that the logic circuitry, for the negative slope case, will measure the range difference between the first and two subsequent readings, covering a total travel distance of 0.5 meters. As a starting point, a detection probability of 98% for 1 meter holes on smooth mare terrain is assumed. A one meter hole will produce a range increase of 1.1 meters in the first 0.50 meters of travel. Thus for 98% detection probability the threshold is set at 2σ below 1.1 meters or .850 meters. Half meter deep, by 1 meter long holes will give a change of 0.7 meters in 0.5 meters of travel and therefore have a false alarm rate of 11%. As mentioned previously, 35° negative slopes (which do not constitute hazards) will not be detected due to weak signal returns and therefore will be recorded as hazards. Furthermore, 25° slopes, which give a range increase of .615 meters in an interval of 0.5 meters of travel will have a false alarm rate of 2.5%.

The same calculations have been carried out for positive and negative obstacles occurring in the rough mare, hummocky upland and rough upland. The results for the four lunar surface categories are summarized in Table 2.

A. 3. 3 The Change of Slope

Additional detection problems will arise when the terrain changes slope angle, from one angle to another. For example, consider Figures 23 & 24 where 4 illustrative cases are shown.

Case A

In this case the vehicle is on a 20° positive slope and is approaching a 15° positive slope with respect to the given slope. Stated otherwise, it is approaching a 35° positive slope, (with respect to level terrain) which constitutes a hazard. However, the radar sees only a 15° slope. In the discussion, concerning positive slopes, (section A-1) it was stated that when the range difference exceeds the threshold value of .77 meters in 1.75 meters of travel (positive slope logic) then the system will indicate a hazard. A 15° slope represents a range change of only $\frac{1.75 \times \sin(15^\circ)}{\sin(60^\circ)}$ or .495 meters in 1.75 meters of travel. Thus, it will have only a 1.5% probability of being detected, assuming a 1σ range error of .125 meters (smooth mare). It is evident, therefore that the threshold value will have to be varied in accordance with the particular slope that the vehicle is on at the moment. For example, for this case, if the threshold were effectively changed to .370 meters by adding a range decrease bias of .400 meters the probability of detecting the 15° slope would be increased to 84%. Referring to Table 2, this value is equivalent to the probability of detecting a 35° positive slope when approached from a flat terrain in the rough uplands.

TABLE 2

SUMMARY OF DETECTION PROBABILITIES AND FALSE ALARM RATES

	Smooth Mare		Rough Mare		Hummocky Upland		Rough Upland	
	Detect. Prob.	False Alarm Rate	Detect. Prob.	False Alarm Rate	Detect. Prob.	False Alarm Rate	Detect. Prob.	False Alarm Rate
1 meter block	99.5%		98%		95%		91%	
1/2 meter block		24%		30%		32%		37%
35° pos slope	98%		93%		90%		84%	
20° pos slope		20%		25%		30%		34%
1 meter hole	98%		93%		90%		84%	
1/2 meter hole		11%		19%		24%		28%
35° neg slope		100%		100%		100%		100%
25° neg slope		2.5%		7%		11%		17%

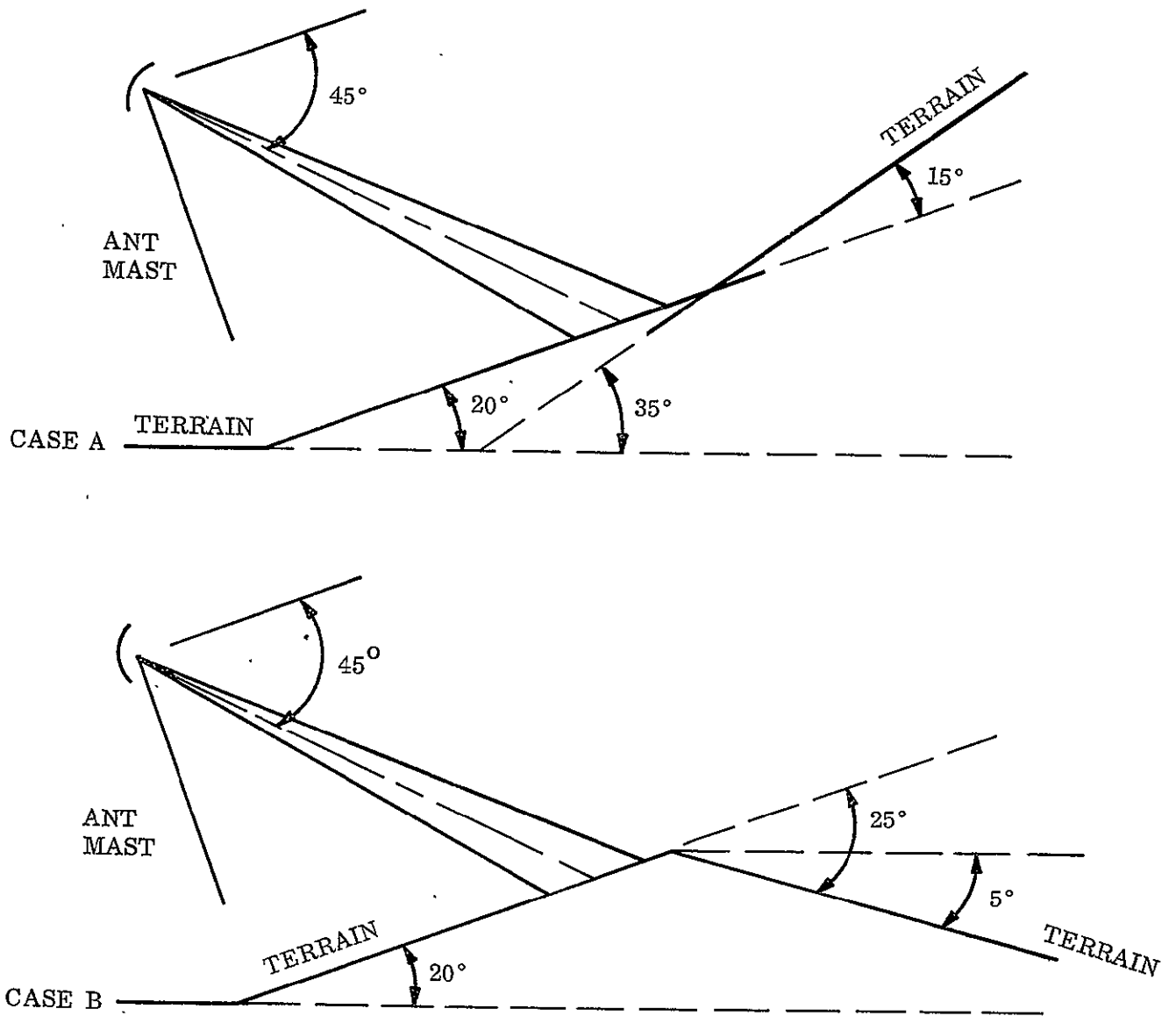


Figure 23. Vehicle Approaching Change of Slope

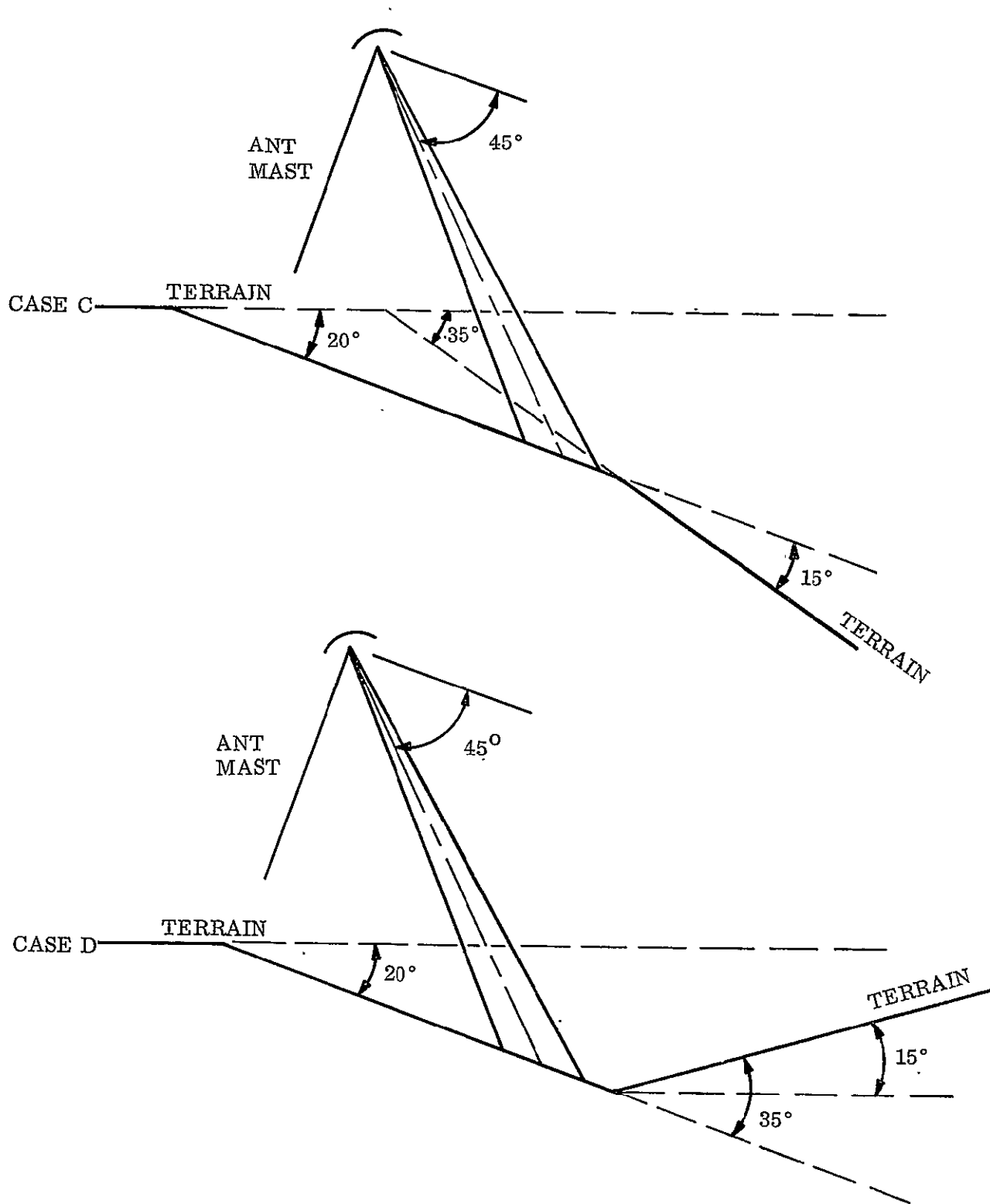


Figure 24. Vehicle Approaching Change of Slope

Case B

In this case the vehicle is on a 20° positive slope and is approaching a 25° negative slope with respect to the given slope (5° slope with respect to the level terrain and therefore non hazardous). Two factors are in operation now. Since the vehicle is on a positive slope the threshold value will have changed by .400 meters in the negative direction (due to range decrease). On the other hand, since the radar is tracking a negative slope, negative slope logic will be in operation. In the discussion concerning negative slopes it was stated that when the range increase exceeds the threshold of .85 meters per 1/2 meter of travel or less, the system will indicate a hazard. A 25° negative slope represents a range increase of $\frac{0.5 \times \sin 25^\circ}{\sin 20^\circ}$ or .615 meters per 1/2 meter of travel. Since the threshold has been changed by .400 meters in the negative direction, the effective range increase is .615 - .400 or .215 meters. Therefore its false alarm rate is less than 0.1%. Referring to Table 2, this value is much less than the false alarm rate caused by 25° negative slopes when approached from a flat terrain in all types of lunar terrain.

Case C

In this case the vehicle is on a 20° negative slope and is approaching a 15° negative slope with respect to the given slope (35° negative slope with respect to level terrain and therefore a hazard). However, the radar sees only a 15° negative slope. A 15° negative slope represents a range increase of $0.5 \times \frac{\sin 15^\circ}{\sin 30^\circ}$ or .253 meters per 1/2 meter of travel. Thus, it will have less than a 1% chance of being detected, assuming the threshold is at .85 meters (negative slope logic). Therefore, as in Case A, the threshold will have to be varied. In this case, if the threshold were effectively changed to .253 meters by adding a range increase bias of .597 meters the detection probability would increase to 50%. Referring to Table 2, this value exceeds the probability of detecting 35° negative slopes when approached from a flat terrain in all types of lunar terrain.

Case D

In this case the vehicle is on a 20° negative slope and is approaching a positive 35° slope. (15° positive slope with respect to level terrain and therefore non hazardous). As in Case B, two factors are now in operation. Since the vehicle is on a negative slope (Case C above) the threshold will have changed by .597 meters in the positive direction (due to range increase). On the other hand, since the radar is tracking a positive slope, positive slope logic will be in operation. As mentioned in Case A, the positive slope logic is such that when the range decrease exceeds the threshold value of .77 meters per 1.75 meters of travel or less the system will indicate a hazard. A 35° positive slope represents a range

decrease of $\frac{1.75 \times \sin 35^\circ}{\sin 80^\circ}$ or 1.02 meters per 1.75 meters of travel. Since the threshold has been changed by .597 meters in the positive direction, the effective range decrease is $1.02 - .597$ or .423 meters. Therefore its false alarm rate is less than 1%. Referring to Table 2, this value is much less than the false alarm rate caused by 20° positive slopes when approached from a flat terrain in all types of lunar terrain.

The foregoing analysis serves to show that changing slopes in the lunar terrain present a serious problem to an automatic hazard detection system. Automatic adjustment of threshold biasing must be incorporated into the system so that detection probability and false alarm rates can be maintained at acceptable levels. Signals to initiate changes in threshold bias must be provided by accurate and reliable attitude sensors.

